High-Performance Flexible Micro-Supercapacitors with Wide Working Voltage Window and Good Durability

Rabah BOUKHERROUB

rabah.boukherroub@univ-lille.fr

http://www.iemn.univ-lille.fr/

By high speed train ...

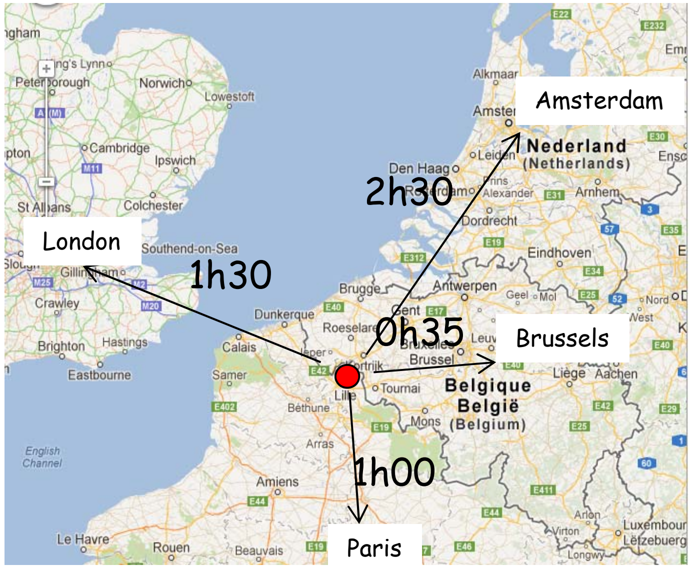

iemn
Institut d'Electronique, de Microélectronique et de Nanotechnologie
UMR CNRS 8520

The research carried out can be divided into six major scientific areas (22 research groups)

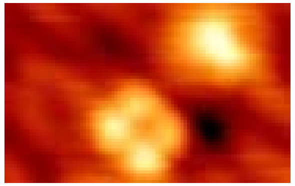

Materials and Nanostructures

Micro- and Nano-systems

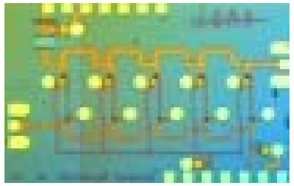

Micro Nano Opto-Electronics

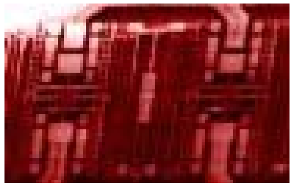

Telecommunication circuits and systems

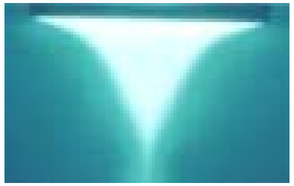

Acoustics

Instrumentation

iemn
Institut d'Electronique, de Microélectronique et de Nanotechnologie
UMR CNRS 8520

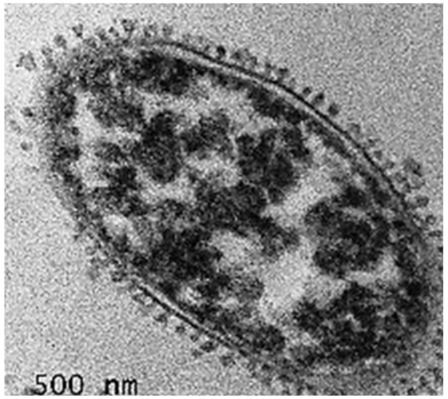

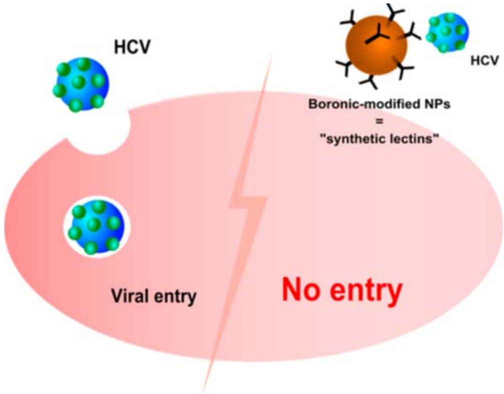

The main projects are:

- **Synthesis of nanostructured materials (nanoparticles, nanowires, nanorods,….) for drug delivery, fighting antibacterial resistance, antivirals, anti-fungal, as potent adjuvants,….**
- **Controlled surface chemistry for specific immobilization of biological molecules**
- **Biomolecule analysis (DIOS-MS)**
- **Label-free detection of biomolecular interactions (SPR, LSPR, electrochemical)**
- **Environmental remediation (photocatalysis, AOPs, adsorption), CO_2 photoreduction**
- **Energy storage (supercapacitors)**
- **Clean energy (water splitting)**

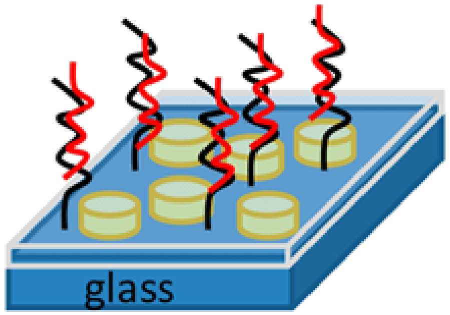

et de Nanotechnologie
UMR CNRS 8520

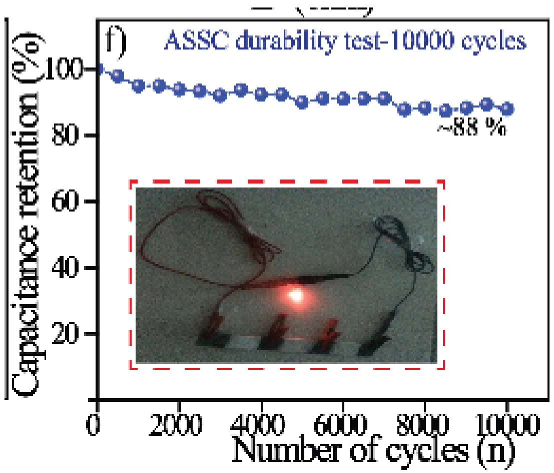

65,673 results from Web of Science Core Collection for:

"supercapacitors" (All Fields)

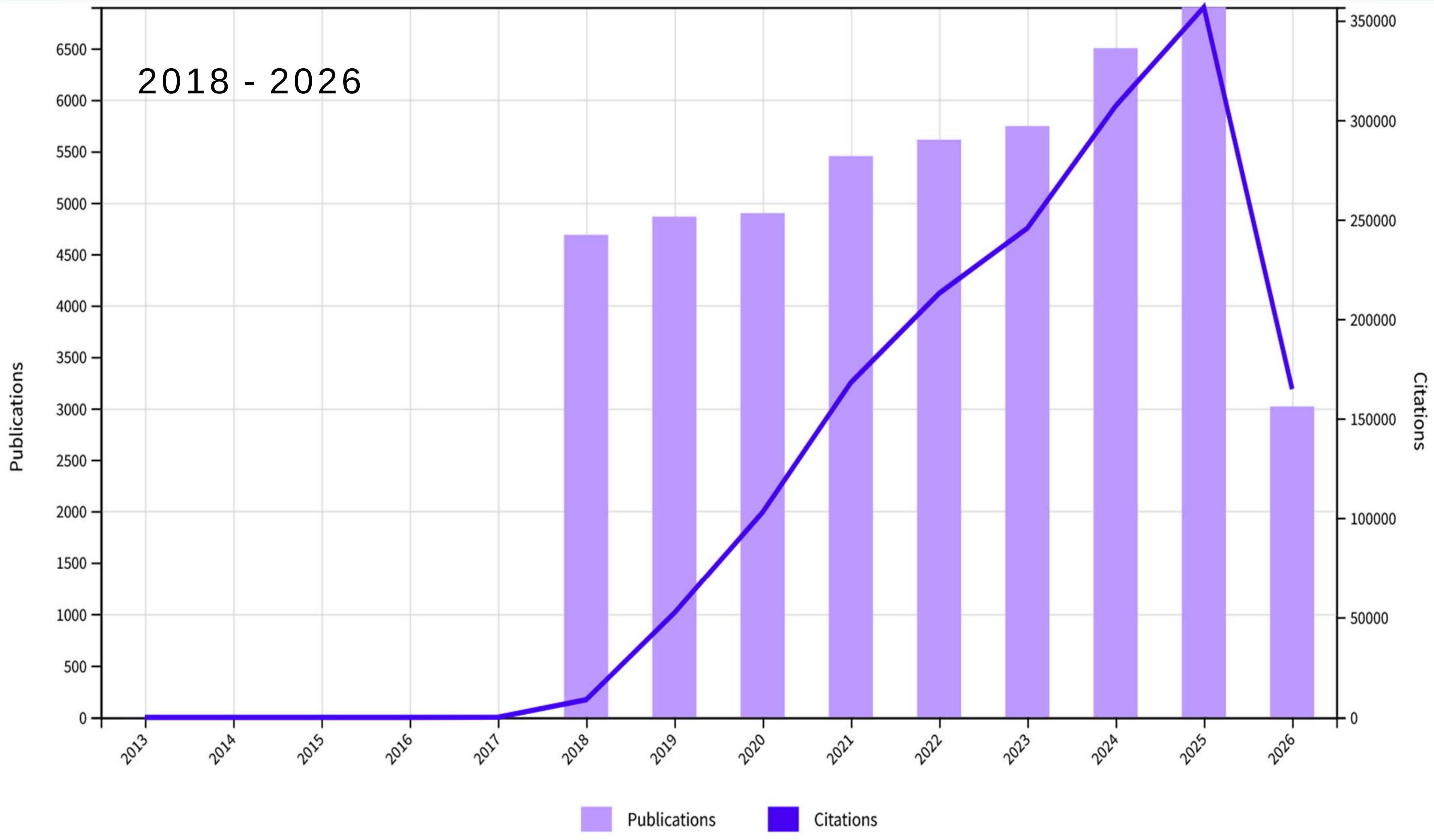

Need for Energy Storage Devices

Depletion of fossil fuels

Population explosion

Environmental pollution

Global warming

It is imperative to develop clean, efficient and sustainable energy sources

Sustainable Living Through Renewable Energy

Wind energy

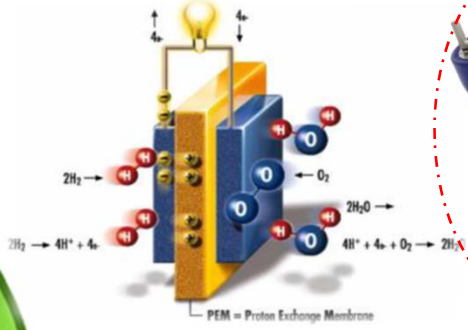

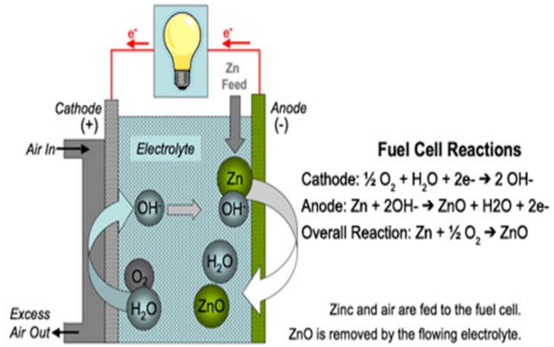

Tidal energy

Geothermal energy

Solar energy

iemn
Institut d'Electronique, de Microélectronique et de Nanotechnologie
UMR CNRS 8520

Batteries *vs.* Supercapacitors

	Batteries	Supercapacitors
Energy Storage Mechanism	Intercalation/de-intercalation of cations (H^+ or Li^+) within the crystalline structure of electrode materials	high-speed electrostatic (EDLCs) or Faradaic electrochemical processes at/or near the electrode surface (Pseudocapacitors)
Recharge Cycle Life Time	$<10^3$ cycles	$>10^6$ cycles
Voltage	3.7-4.2 V	0-2.7 V
Energy Density (Wh kg^{-1})	high (20-250)	low (0.8-10)
Power Density (W kg^{-1})	low (50-300)	high (400-500)
Charging Time	hours	sec ~ min
Lifetimes	limited by redox irreversibility & phase changes	long lifetimes

Wide Operating Temperature Range

Environmental Friendliness

iemn
Institut d'Electronique, de Microélectronique et de Nanotechnologie
UMR CNRS 8520

Supercapacitors - Target

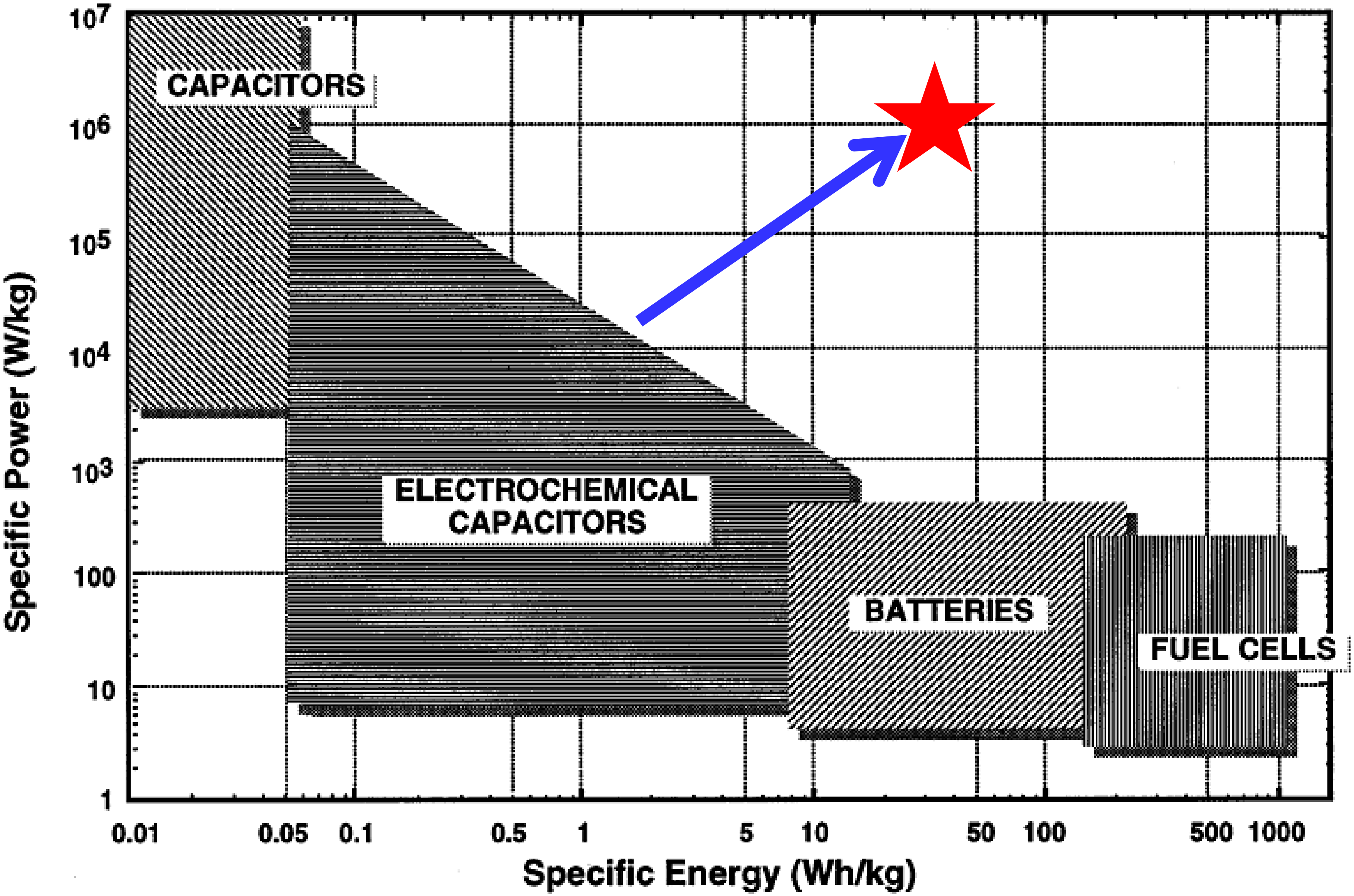

Development of Capacitors and Supercapacitors

Electrical double layer capacitors (EDLC) patent — 1957

RuO_2 pseudo-capacitors — 1975-1980

Hybrid supercapacitors — 1990s

Nowadays:
Replace batteries in some applications

1950 1960 1970 1980 1990 2000 2010 2020

Hybrid supercapacitor ($AC//Ni(OH)_2$), used in the fast charge e-bus, could be fully charged within 90 s.

Charged at the bus stop station

iemn
Institut d'Electronique, de Microélectronique et de Nanotechnologie
UMR CNRS 8520

ESs with improved performance and low production cost should be developed

Conventional Capacitors *vs.* electrochemical supercapacitors

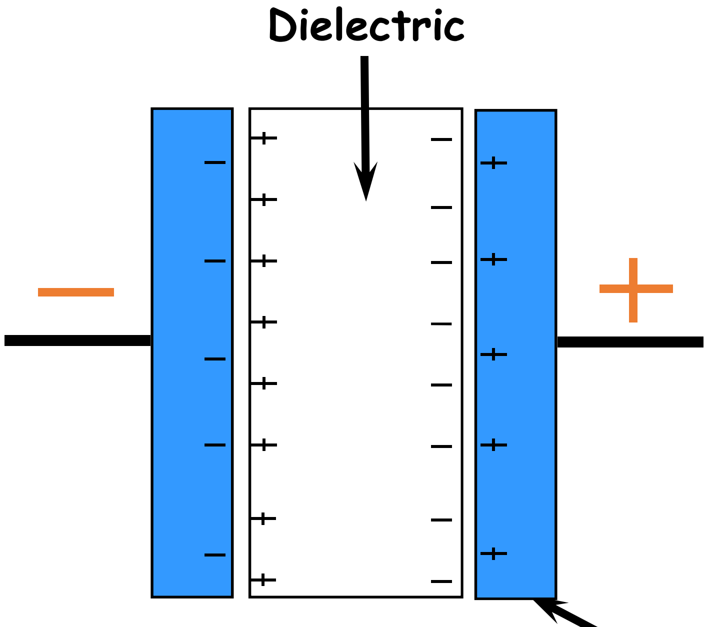

$C = e_r\, A/d$

Minimise (d)

Maximise (A)

$E = 1/2\, CV^2$

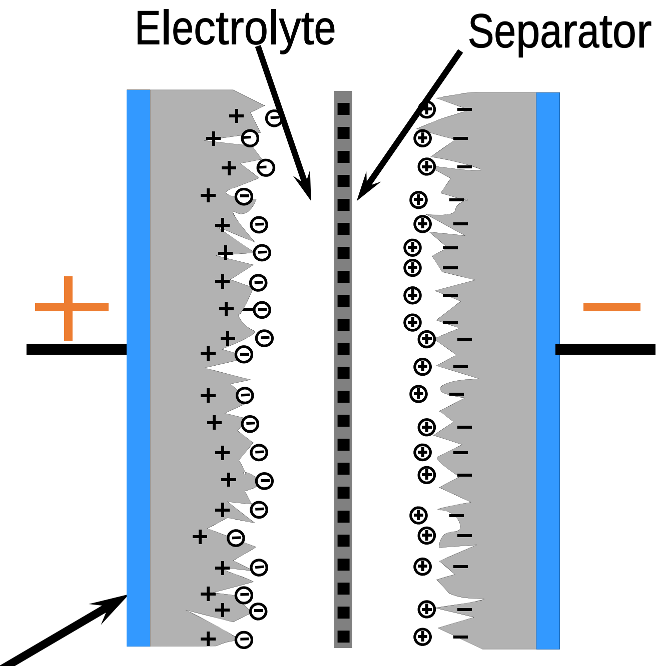

Electrode

Conventional Capacitor

$$C\ (\mathrm{mF{\cdot}cm^{-2}}) = \frac{I \times \Delta t}{A \times \Delta V}$$

Supercapacitor

iemn
Institut d'Electronique, de Microélectronique et de Nanotechnologie
UMR CNRS 8520

Electric Double Layer Capacitors

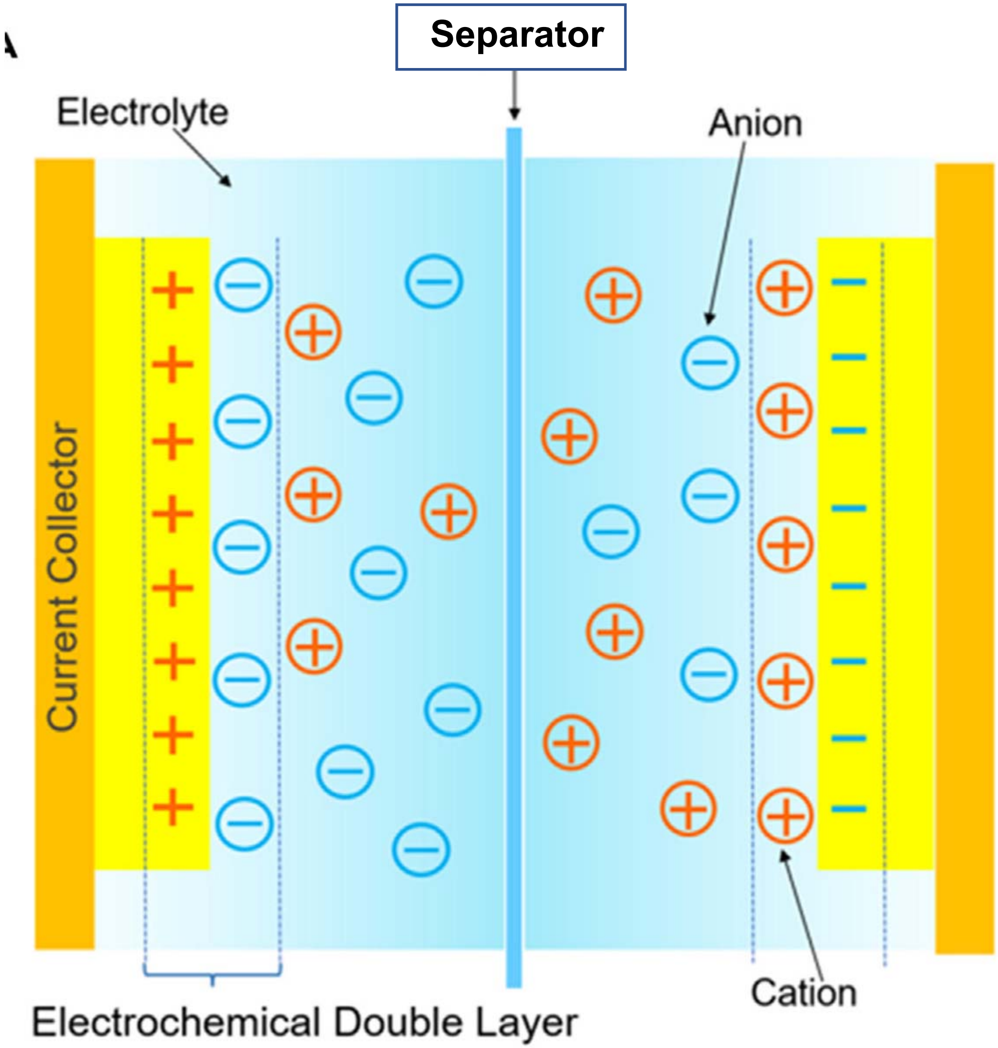

iScience 27, 108786, February 16, 2024

Pseudocapacitors

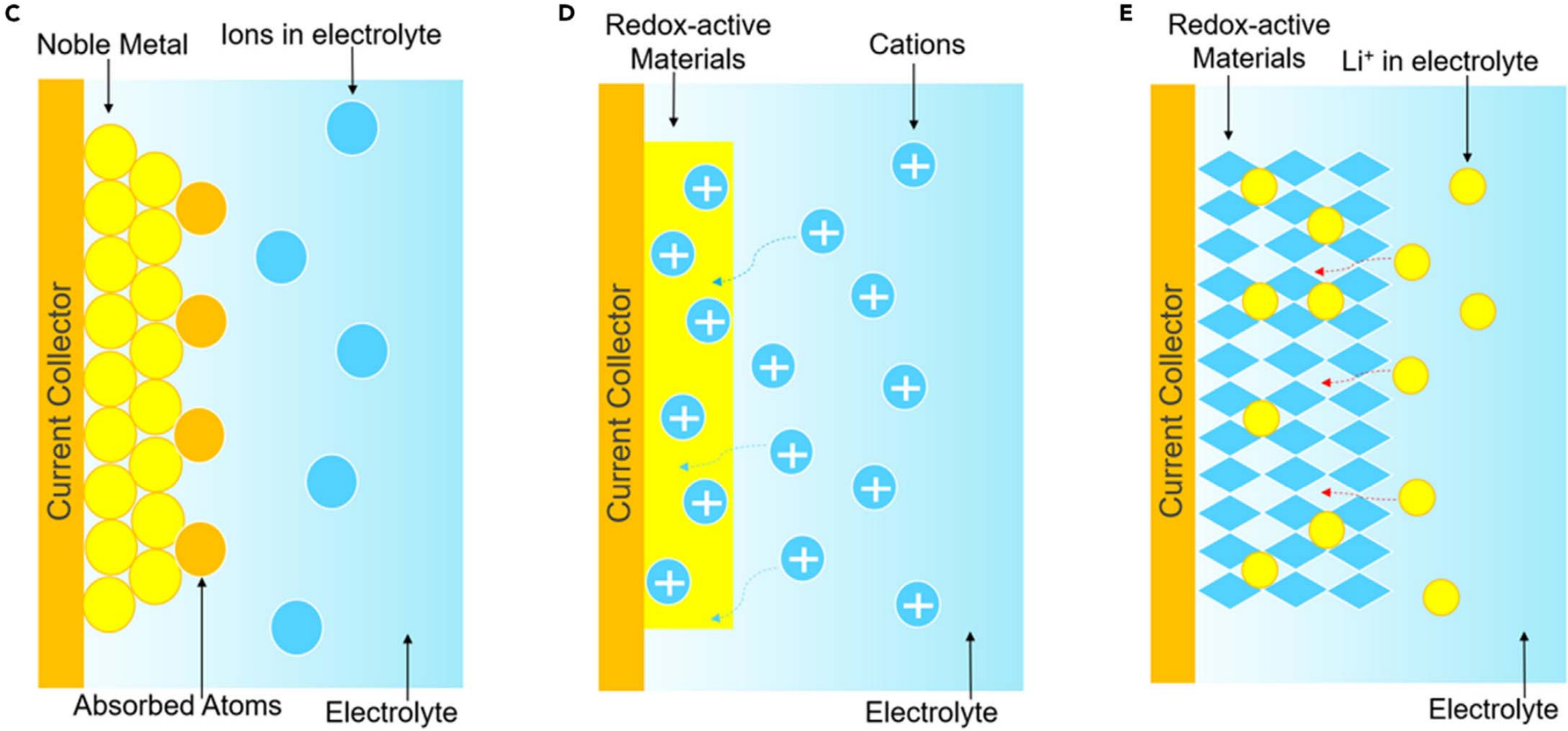

iemn
Institut d'Electronique, de Microélectronique et de Nanotechnologie
UMR CNRS 8520

iScience 27, 108786, February 16, 2024

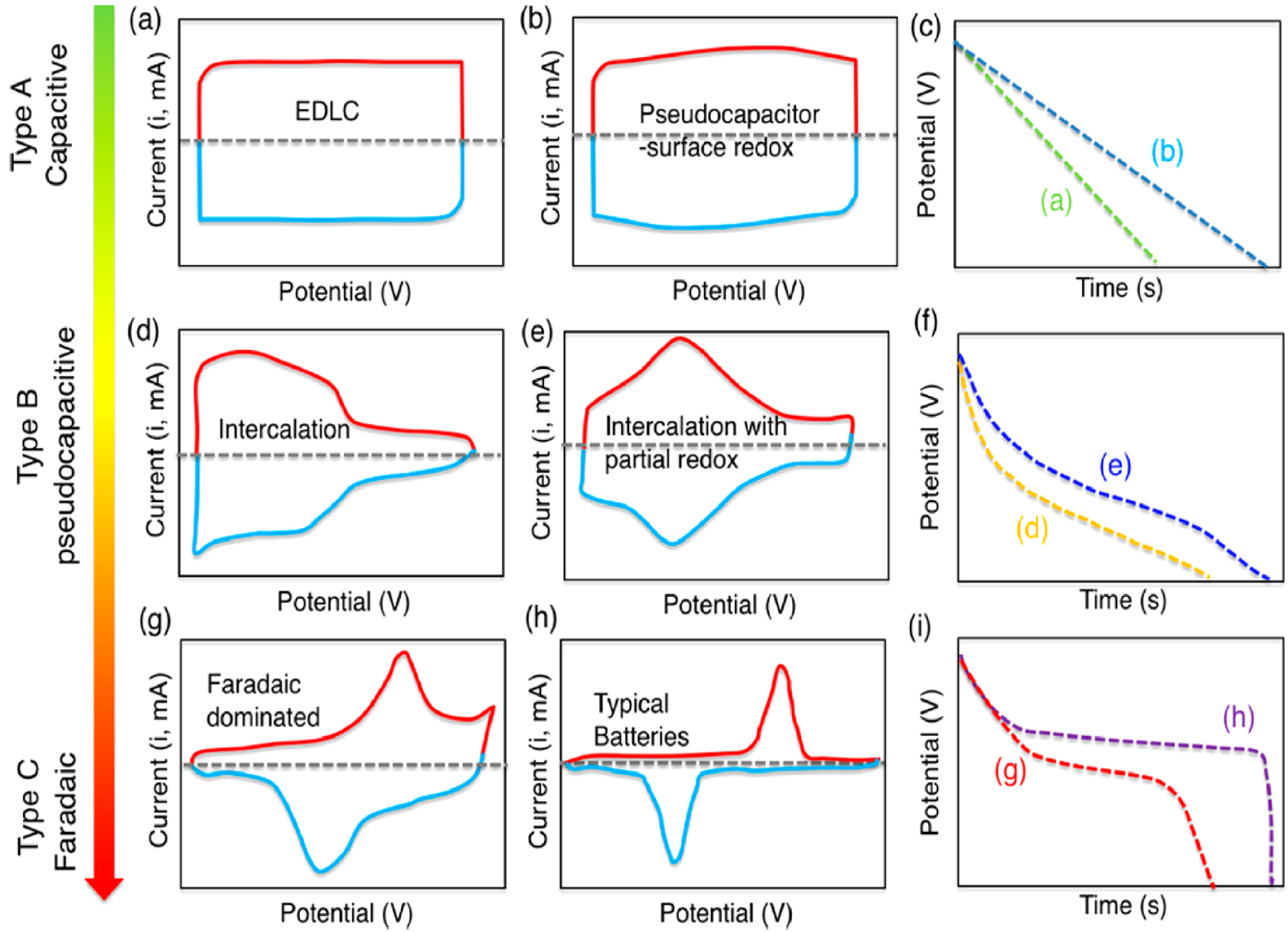

CV GCD

iemn
Institut d'Electronique, de Microélectronique et de Nanotechnologie
UMR CNRS 8520

Suitable Electrode Materials

- Reasonable high conductivity
- Relatively high surface-area
- Excellent corrosion resistance
- High thermal stability
- Controlled pore size distribution
- Satisfactory compatibility in composite materials
- Cost effectiveness
- Biocompatibility

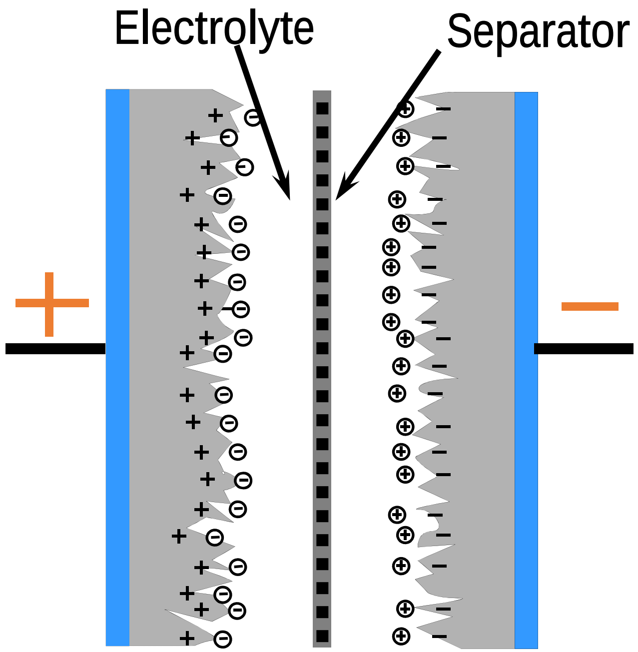

iemn
Institut d'Electronique, de Microélectronique et de Nanotechnologie
UMR CNRS 8520

Structure and Classification

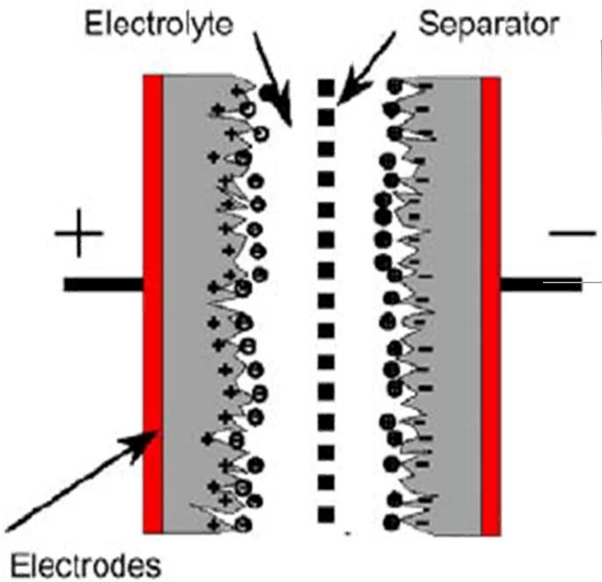

Electric Double Layer Capacitors (EDLCs)

Reversible electrostatic charge adsorption at the electrode-electrolyte interface

- Carbon-based materials

Pseudocapacitors

Rapid reversible faradaic redox reactions in the surface or near surface of the electrode materials

- Transition metal oxides / hydroxides / sulfides / nitrides
- Conductive polymers

Asymmetric Supercapacitors

- Capacitive asymmetric SCs (Capacitive/capacitive)
- Hybrid supercapacitors (Faradaic/capacitive)

The choice of negative electrodes

Negative electrodes

Mesoporous carbon (MC)

- High specific surface area (>200 m^2 g^{-1})
- Effective conductivity

Nitrogen-doped reduced graphene oxide (N-rGO)

- Excellent electrical conductivity
- High theoretical specific surface area (~2620 m^2 g^{-1} for graphene)

Ferric oxyhydroxide (FeOOH)

- Good conductivity
- Being abundant
- Low cost
- Environmental friendliness

iemn
Institut d'Electronique, de Microélectronique et de Nanotechnologie
UMR CNRS 8520

The choice of positive electrodes

Nickel hydroxide ($Ni(OH)_2$)

- High theoretical specific capacitance ($2082\ F\ g^{-1}$)
- Cost-effective
- Stable in alkaline electrolytes
- Available in various morphologies
- Simple synthetic procedure

\+ **CuO**

- One-dimensional (1D) nanowires structure
- Good electrical conductivity
- Low cost
- Simple synthetic procedure

Ni-based layered double hydroxides (LDHs)

- Tunable chemical composition
- Well-defined redox behavior and high redox activity
- Stable in alkaline electrolytes
- Large surface area with exposed atoms
- Low cost

NiFe LDHs → **Fe**

- Being abundant
- Low cost
- Simple synthetic procedure

NiAl LDHs → **Al**

- Good conductivity
- Low cost
- Being abundant
- Simple synthetic procedure

NiMnCr LDHs → **Cr/Mn**

- Plentiful oxidation states (Cr: +1 to +6; Mn:+2 to +7)
- Low cost
- Being abundant (Mn)
- Simple synthetic procedure

Suitable Electrolyte

Aqueous

Eg: aq. solutions of
- H_2SO_4, KOH, Na_2SO_4 NaCl etc.

May have higher C and Power than Organic electrolytes due to higher ionic concentration and smaller ionic radius.

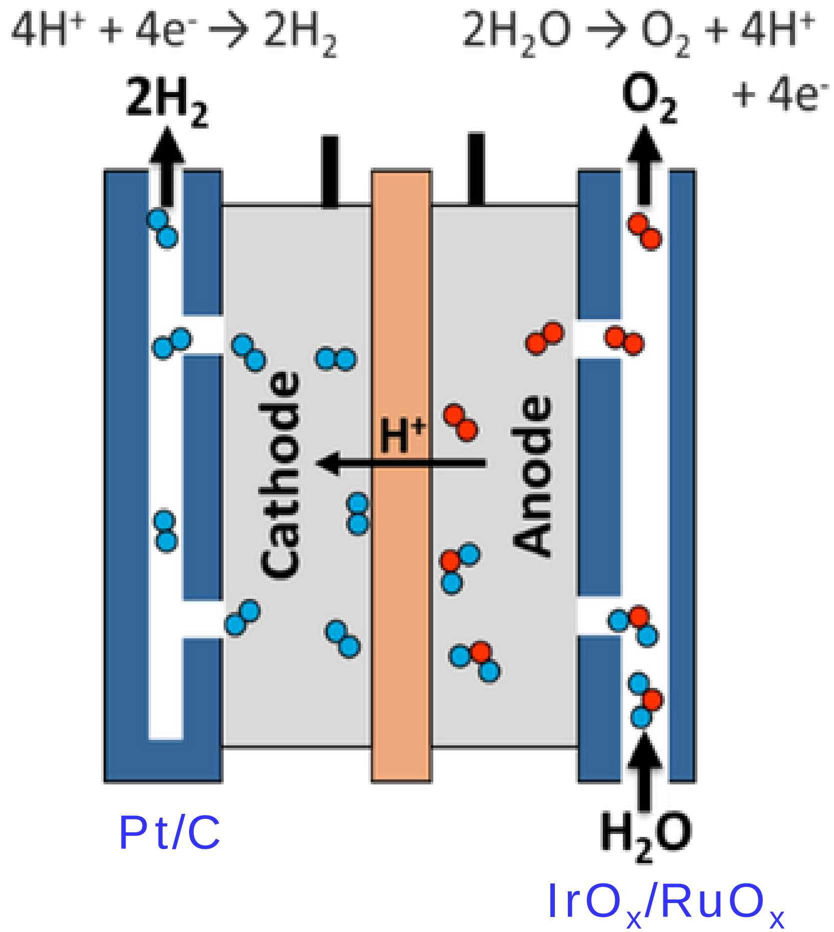

Small voltage window (~1.2 V). Therefore, a big limitation to improve the energy and power densities

Limited operation under harsh environmental conditions

iemn
Institut d'Electronique, de Microélectronique et de Nanotechnologie
UMR CNRS 8520

Suitable Electrolyte

Aqueous	Non-Aqueous	Ionic Liquids
Eg: aq. solutions of - H_2SO_4, KOH, Na_2SO_4 NaCl etc.	Eg: acetonitrile, propylene carbonate, tetraethyl-ammoniumtetrafluoroborate, tetraethylphosphonium tetrafluoroborate, and triethylmethylammonium tetrafluoroborate (TEMABF4)	Eg: imidazolium, pyrrolidinium, as well as asymmetric, aliphatic quaternary ammonium salts with anions such as tetrafluoroborate, trifluoromethanesulfonate etc.
May have higher C and Power than Organic electrolytes due to higher ionic concentration and smaller ionic radius.	Large voltage window (~3.5 V)	Large voltage window (2-6 V). Low flammability, Low vapor pressure etc.
Small voltage window (~1.2V). Therefore, a big Limitation to improve the energy and power densities.	Water content must be kept Very low (3-5 ppm). Otherwise, V may be reduced	Insufficient conductivity is the main problem

Electrochemical measurement metrics

Cyclic Voltammetry (CV)

$$C\text{ (capacity)} = \frac{1}{2mv}\int_{V_1}^{V_2} I(V)\,dV$$

m is the mass loading of electrodes, v is the scan rate, V_1 and V_2 are respectively the low- and high-end potentials, and I (A) is the current

Galvanostatic Charge-Discharge (GCD)

$$C\text{ (capacity)} = \frac{I\,\Delta t}{m}$$

I (A) is the current, Δt is the discharge time, m is the mass loading of electrodes and ΔV is the potential window

$$C\text{ (capacitance)} = \frac{I\,\Delta t}{m\Delta V}$$

Energy Density (E)
Power Density (P)

$$E = \frac{1}{2} C V^2 \qquad P = \frac{E}{\Delta t}$$

C is the capacity, ΔV is the working potential window, *Δt is the discharge time*

Cycling Stability

Overview of micro-supercapacitors (MSCs) parameters, configuration, properties, and application fields

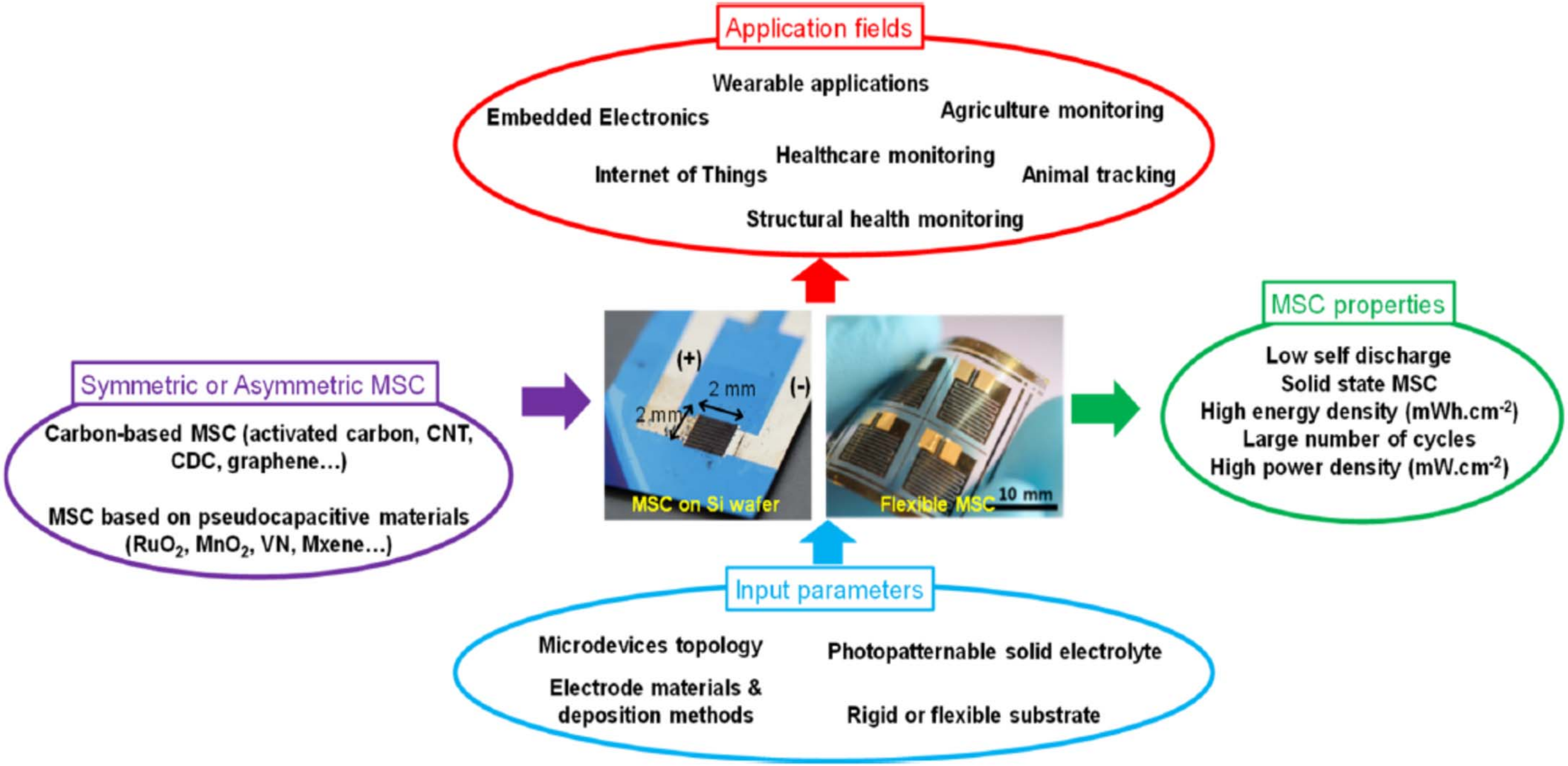

iemn
Institut d'Electronique, de Microélectronique et de Nanotechnologie
UMR CNRS 8520

ACS Omega 2023, 8, 8977−8990

Schematics of the configurations of micro-supercapacitors

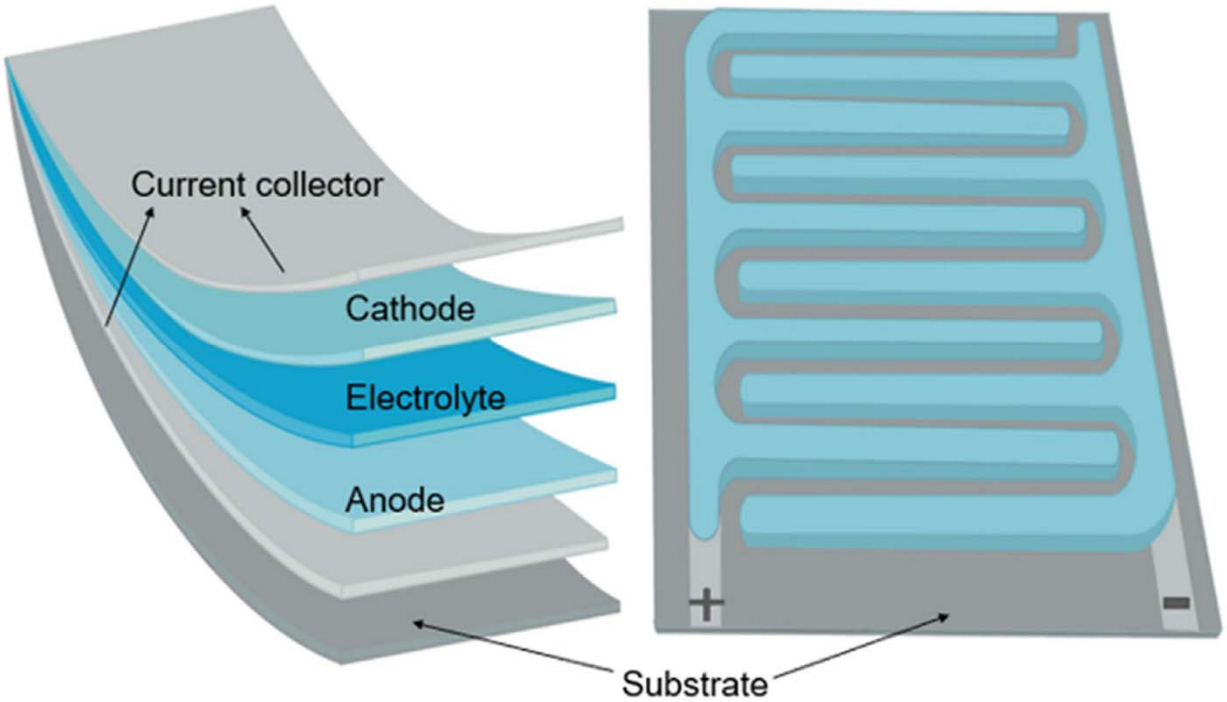

Left: stacked configuration. Micro_supercapacitors are fabricated by depositing the current collector, the first electrode material, solid electrolyte, second electrode material and second current collector consecutively on the same footprint area as the substrate, with a current distribution running perpendicularly to the overall thickness.

Right: planar configuration. Positive and negative electrodes are positioned next to each other on a current collector pre-patterned on an insulating substrate.

iScience 27, 108786, February 16, 2024

Number of publications on micro-supercapacitors according to the Web of Science (as of June 25, 2026)

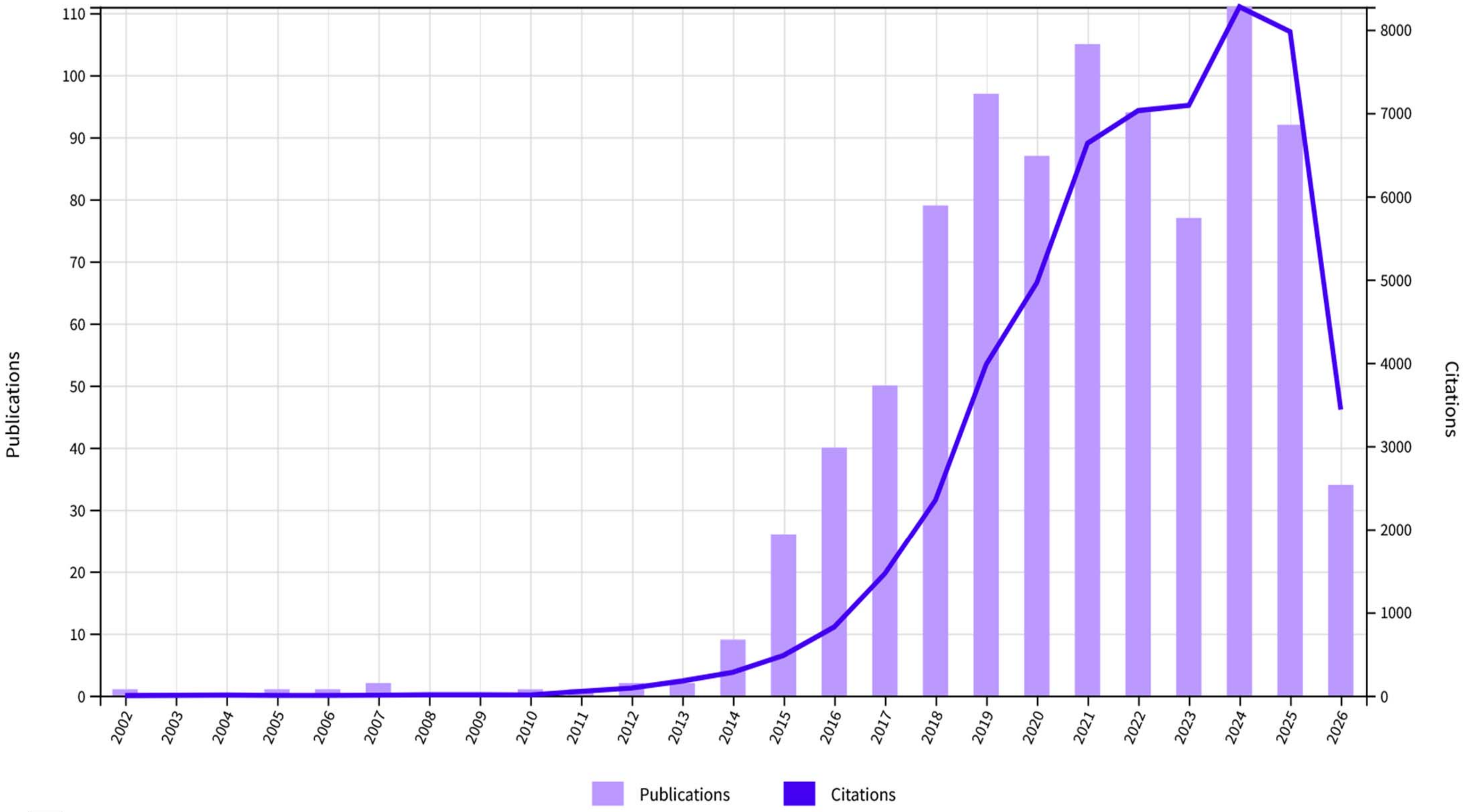

Institut d'Electronique, de Microélectronique et de Nanotechnologie
UMR CNRS 8520

Overview of the fabrication techniques for p-MSCs and their associated benefits

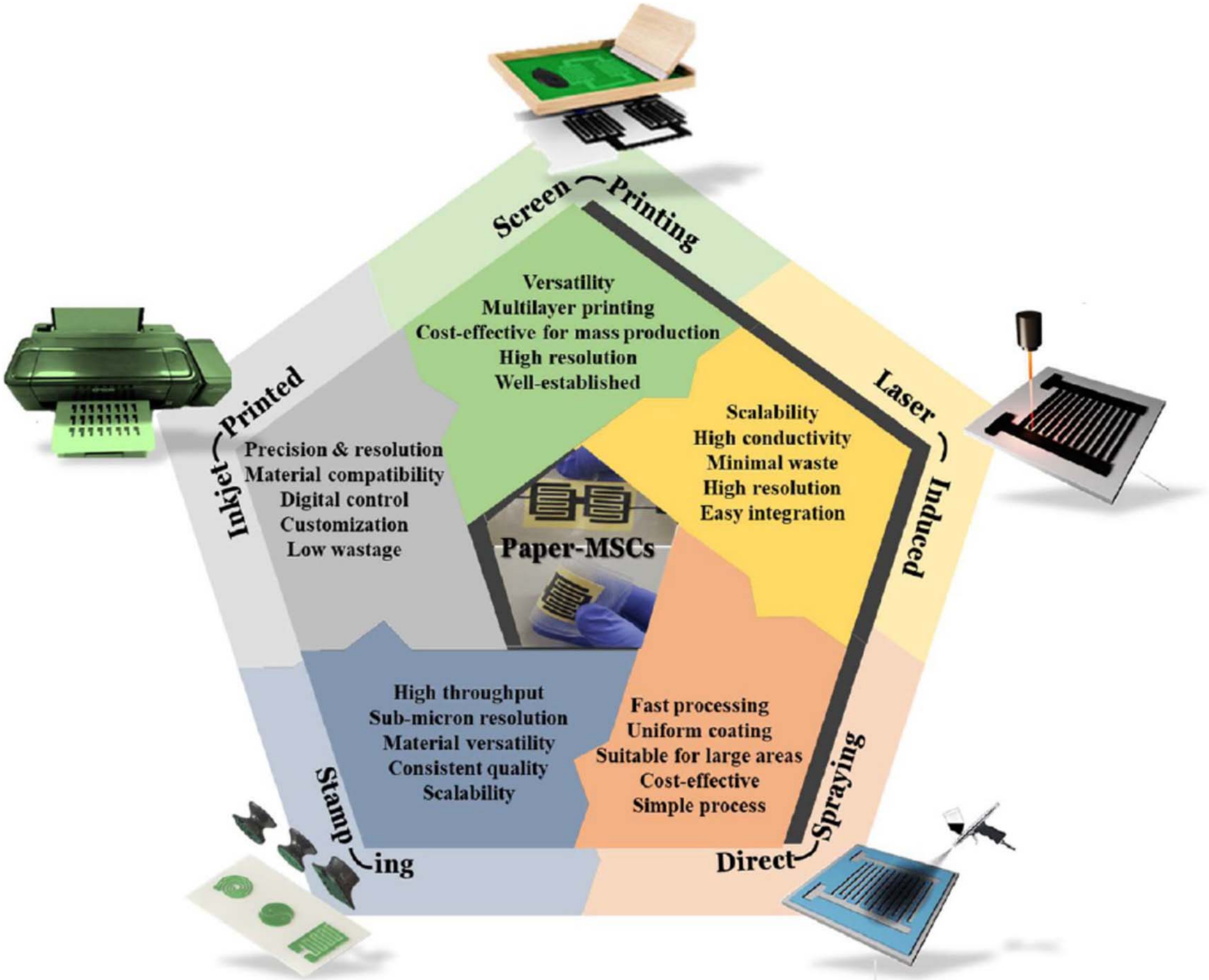

iem
Institut d'Elect
et de Nanotech
UMR CNRS 8520

ACS Appl. Mater. Interfaces **2024, 16, 21367−21382**

A timeline highlighting significant turning points in the development of p-MSCs

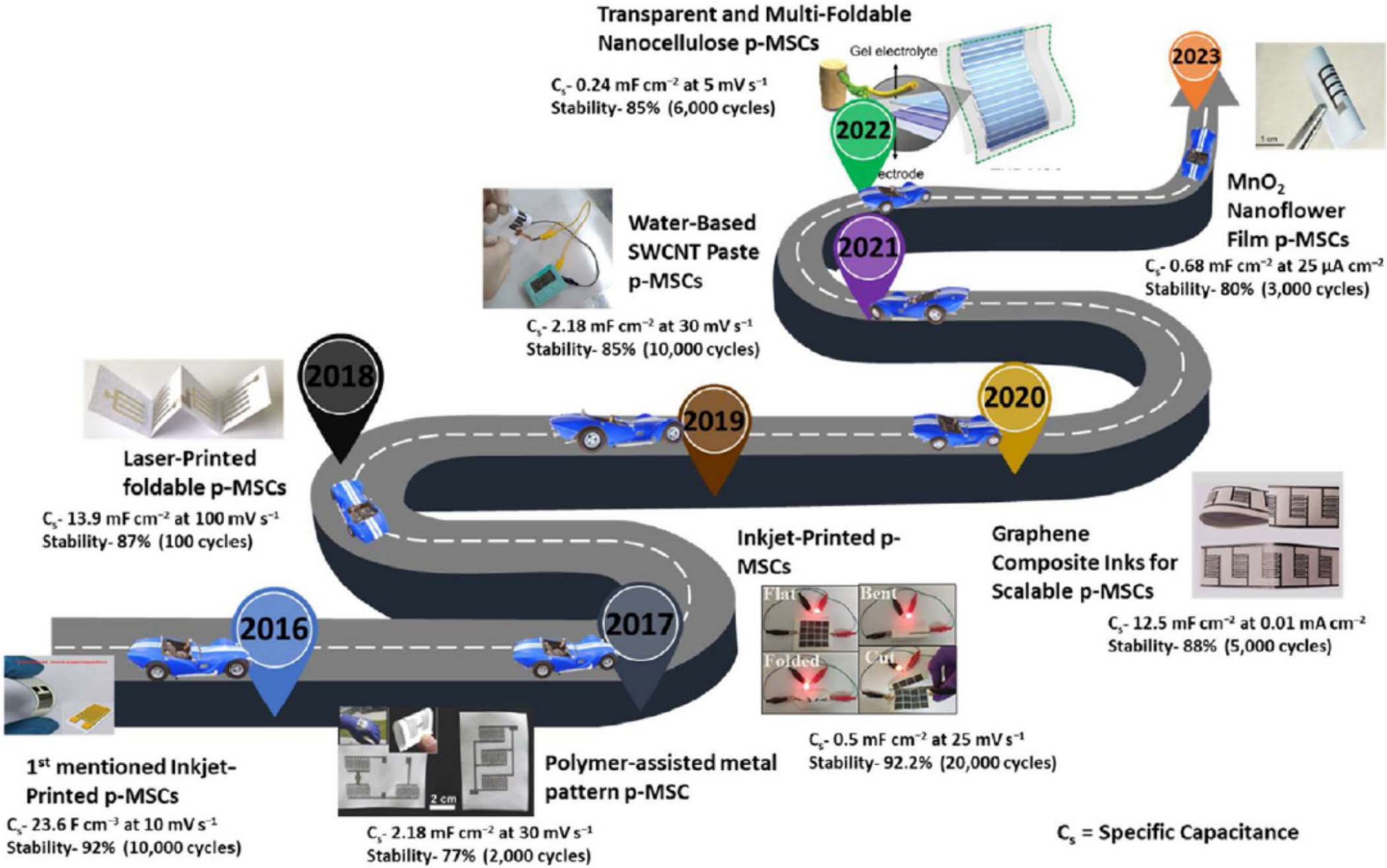

UMR CNRS 8520

ACS Appl. Mater. Interfaces 2024, 16, 21367−21382

Wide-Temperature-Range Flexible Micro-Supercapacitors based on SWCNTs Using Liquid Crystal Gel Electrolyte

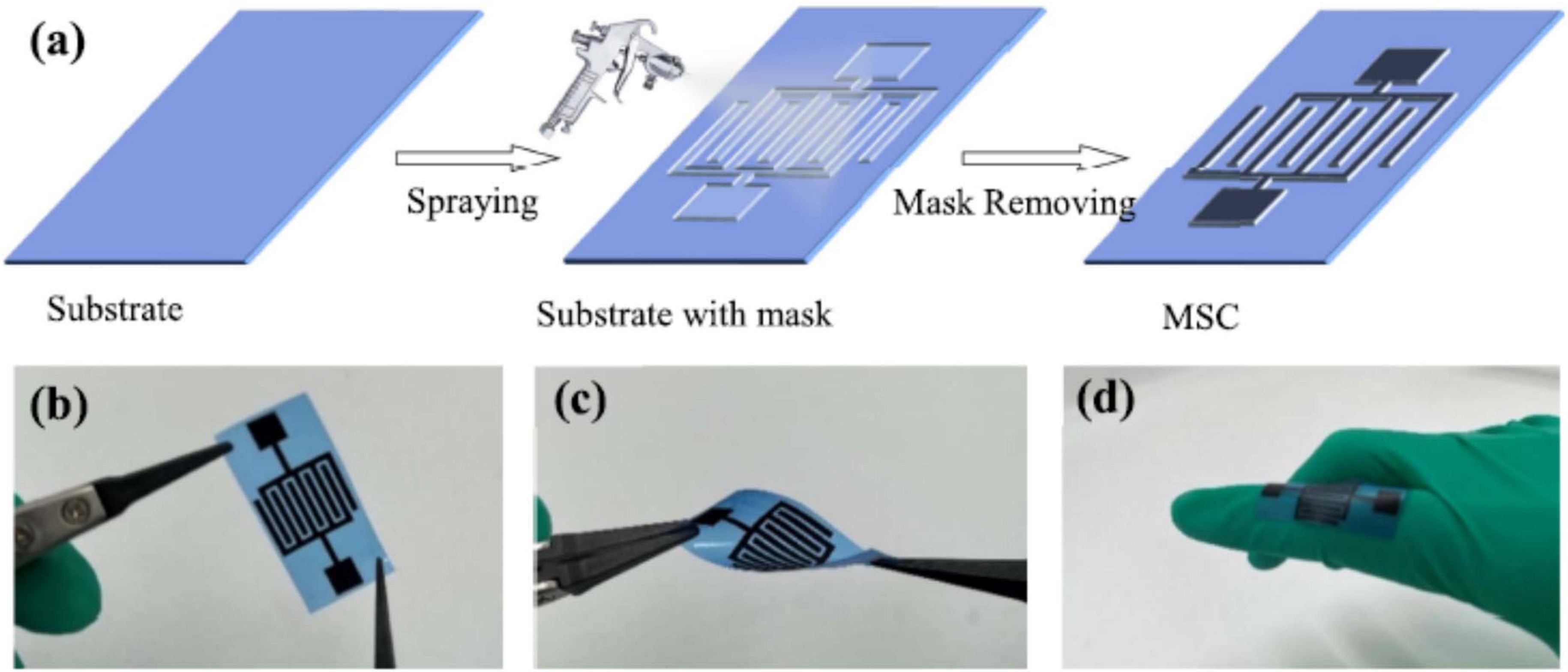

PA-NI LC Gel Electrolyte = Lauryl ether, ($C_{12}H_{25}[OCH_2CH_2]_{10}OH$) + **Phosphoric acid** (H_3PO_4)

iemn
Institut d'Electronique, de Microélectronique et de Nanotechnologie
UMR CNRS 8520

Li et al. *ACS Applied Energy Materials* 6 (**2023**) 5230-5238

Wide-Temperature-Range Flexible Micro-Supercapacitors based on SWCNTs Using Liquid Crystal Gel Electrolyte

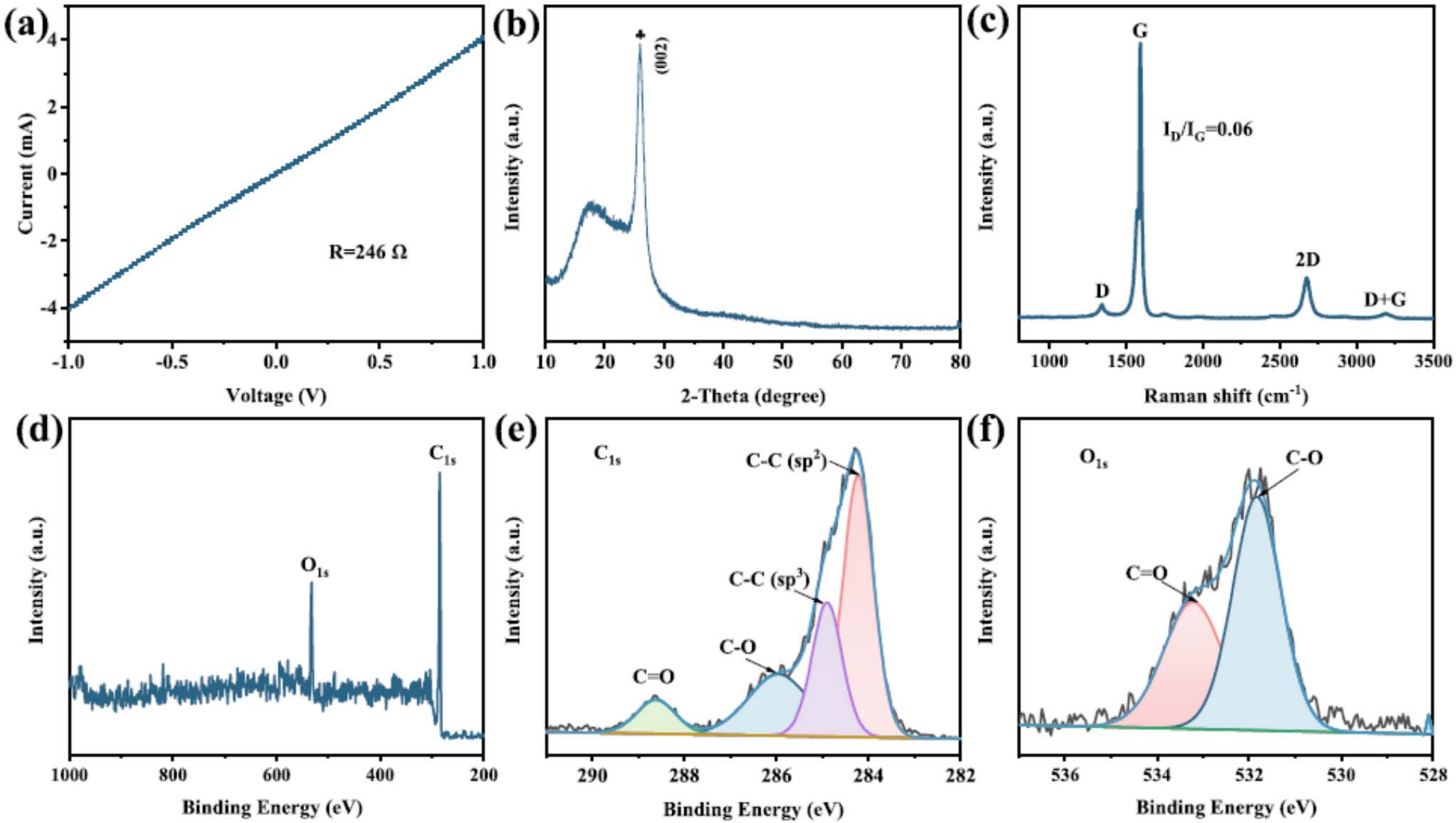

Figure 2. (a) *I*−*V* curve, (b) XRD pattern, (c) Raman spectrum, (d) XPS survey spectrum, and core level spectra of the (e) C_{1s} and (f) O_{1s} of the SWCNTs electrode.

iemn
Institut d'Electronique, de Microélectronique et de Nanotechnologie
UMR CNRS 8520

Li et al. *ACS Applied Energy Materials* 6 (**2023**) 5230-5238

Wide-Temperature-Range Flexible Micro-Supercapacitors based on SWCNTs Using Liquid Crystal Gel Electrolyte

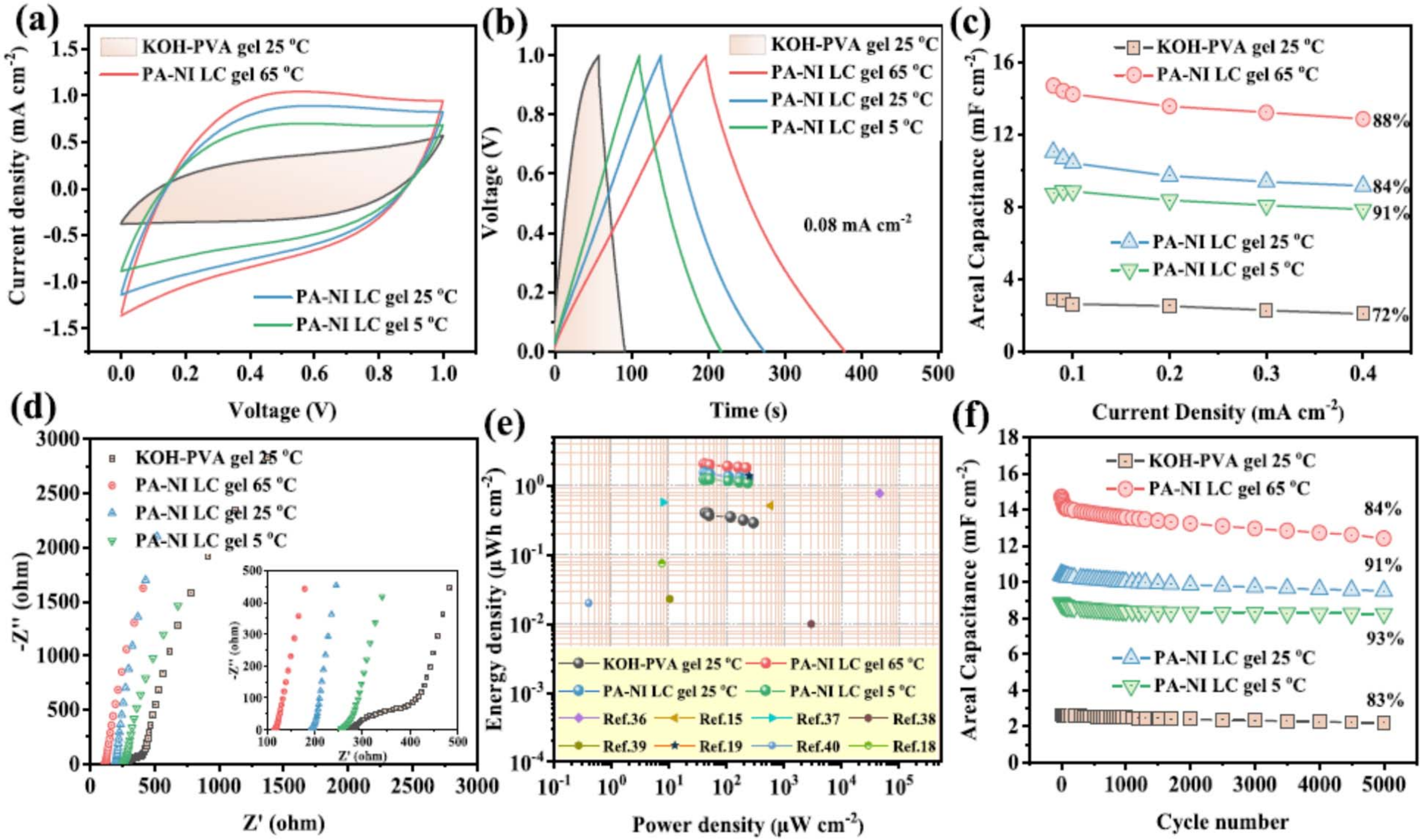

Figure 5. Electrochemical performance of the symmetric SWCNTs//SWCNTs MSCs using PA-NI LC and KOH-PVA gel electrolytes. (a) CV curves recorded at 100 $mV \cdot s^{-1}$, (b) GCD profiles at 0.08 $mA \cdot cm^{-2}$, (c) areal capacitance, (d) electrochemical impedance spectra, (e) Ragone plot, and (f) cycling stability.

iemn
Institut d'Electronique, de Microélectronique et de Nanotechnologie
UMR CNRS 8520

Li et al. *ACS Applied Energy Materials* 6 (**2023**) 5230-5238

Wide-Temperature-Range Flexible Micro-Supercapacitors based on SWCNTs Using Liquid Crystal Gel Electrolyte

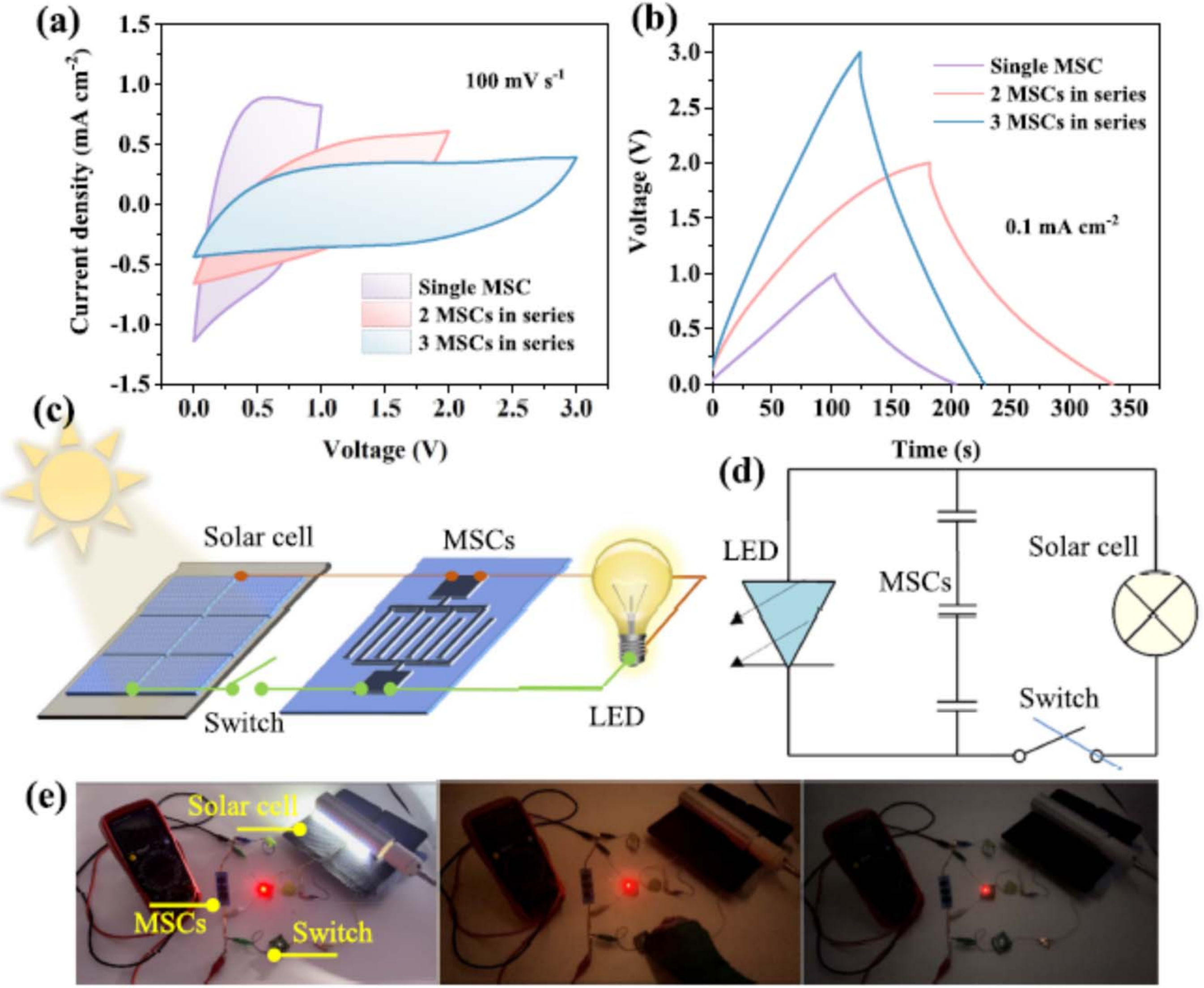

Figure 6. (a) CV curves at 100 mV·s^{-1} of a single MSC, and 2 and 3 SWCNTs/PA-NI LC gel electrolyte MSCs connected in series. (b) GCD plots at 0.1 mA·cm^{-2}. (c) Schematic diagram, (d) equivalent circuit, and (e) photographs of the sunlight-powered energy storage system.

Li et al. *ACS Applied Energy Materials* 6 (**2023**) 5230-5238

Why is laser-induced graphene (LIG) Technique?

2014: 1st introduction for the direct laser writing method to produce LIG

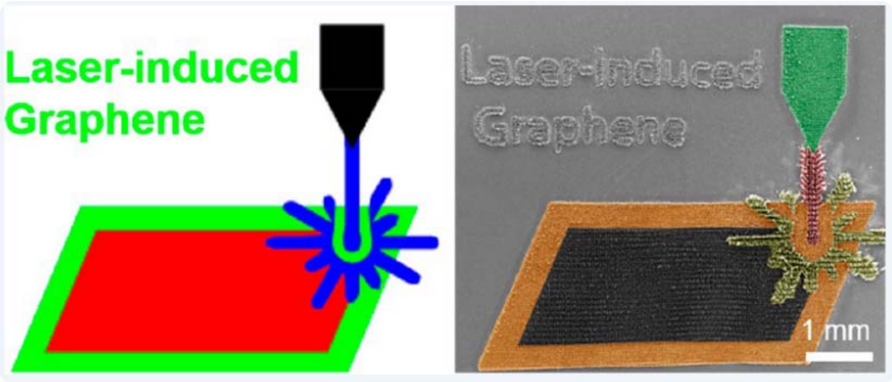

LIG technique offer:

- **Fast**
  - **it achieves both material conversion and electrode patterning in a single step.**
- **Low-Cost**
  - **it does not require high temperatures, solvents and cleanroom conditions.**
- **Tunability**
  - **The laser wavelength, scanning conditions, and substrate material all influence the structure and properties of the resulting LIG.**

James Tour 2014, Rice University

Laser-induced graphene (LIG) Technique

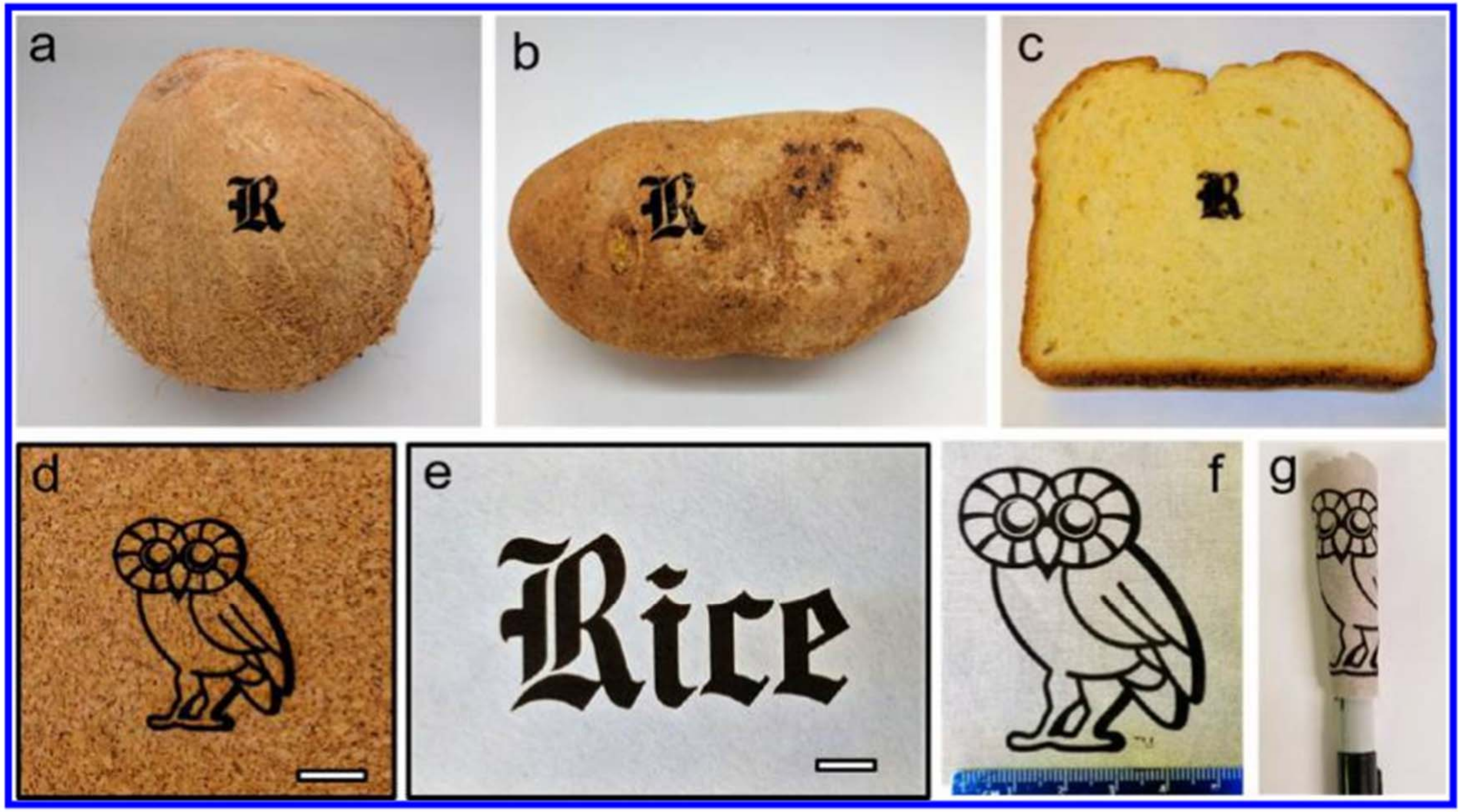

Figure 5. LIG formation on various substrates. Photos of LIG patterned on (a) a coconut, (b) a potato, (c) a piece of bread, (d) a cork, (e) paper, and (f) a muslin cloth. The scale bars are 1 cm. (g) LIG on muslin cloth wrapped around a marker. All owls depicted are 60 mm in height. Adapted

James Tour 2014, Rice University

Flexible Symmetric Micro-Supercapacitors with Wide Working Voltage Window Assisted by Laser Fabrication and Liquid Crystal Gel Electrolyte

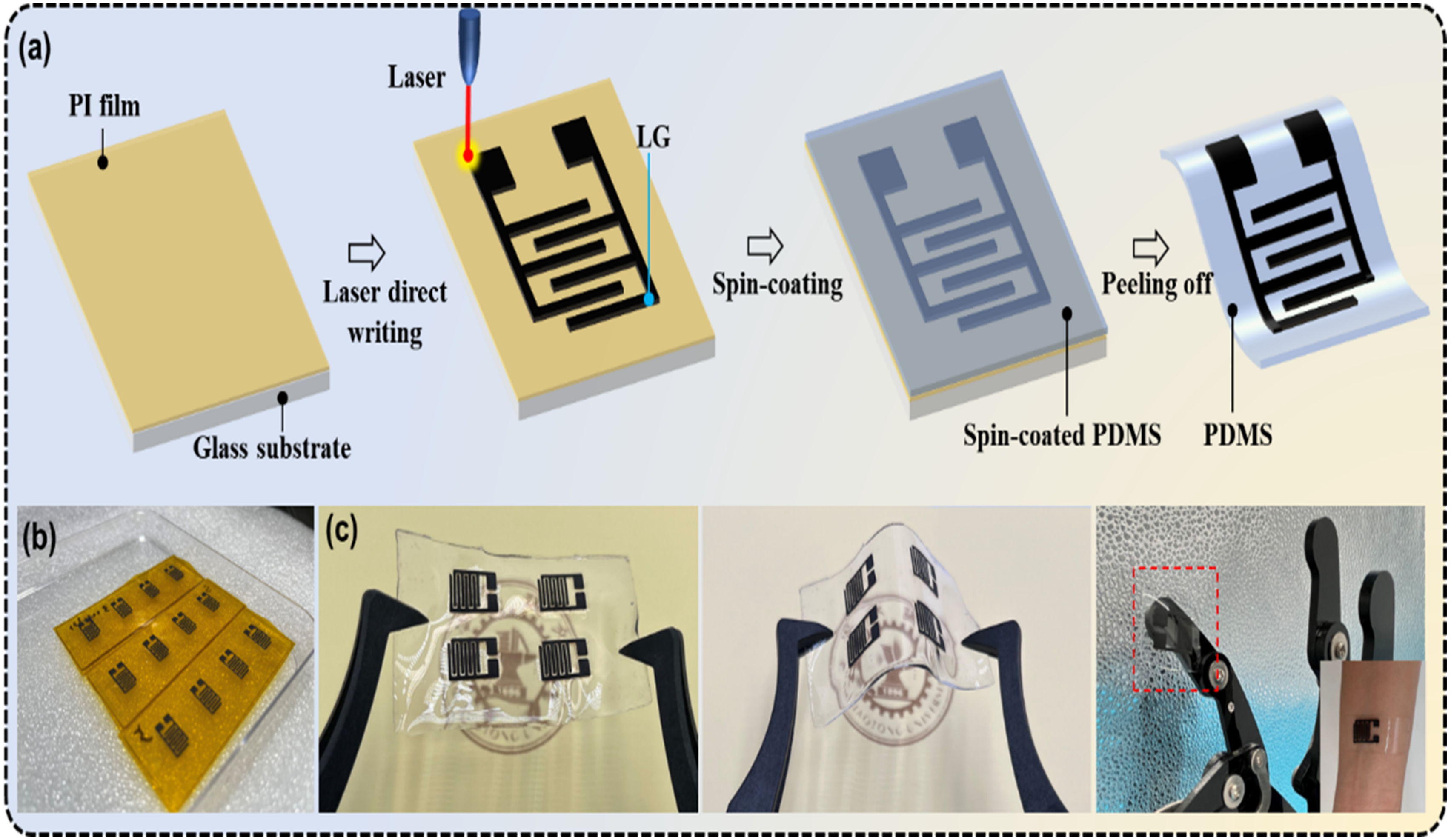

iemn
Institut d'Electronique, de Microélectronique et de Nanotechnologie
UMR CNRS 8520

Flexible Symmetric Micro-Supercapacitors with Wide Working Voltage Window Assisted by Laser Fabrication and Liquid Crystal Gel Electrolyte

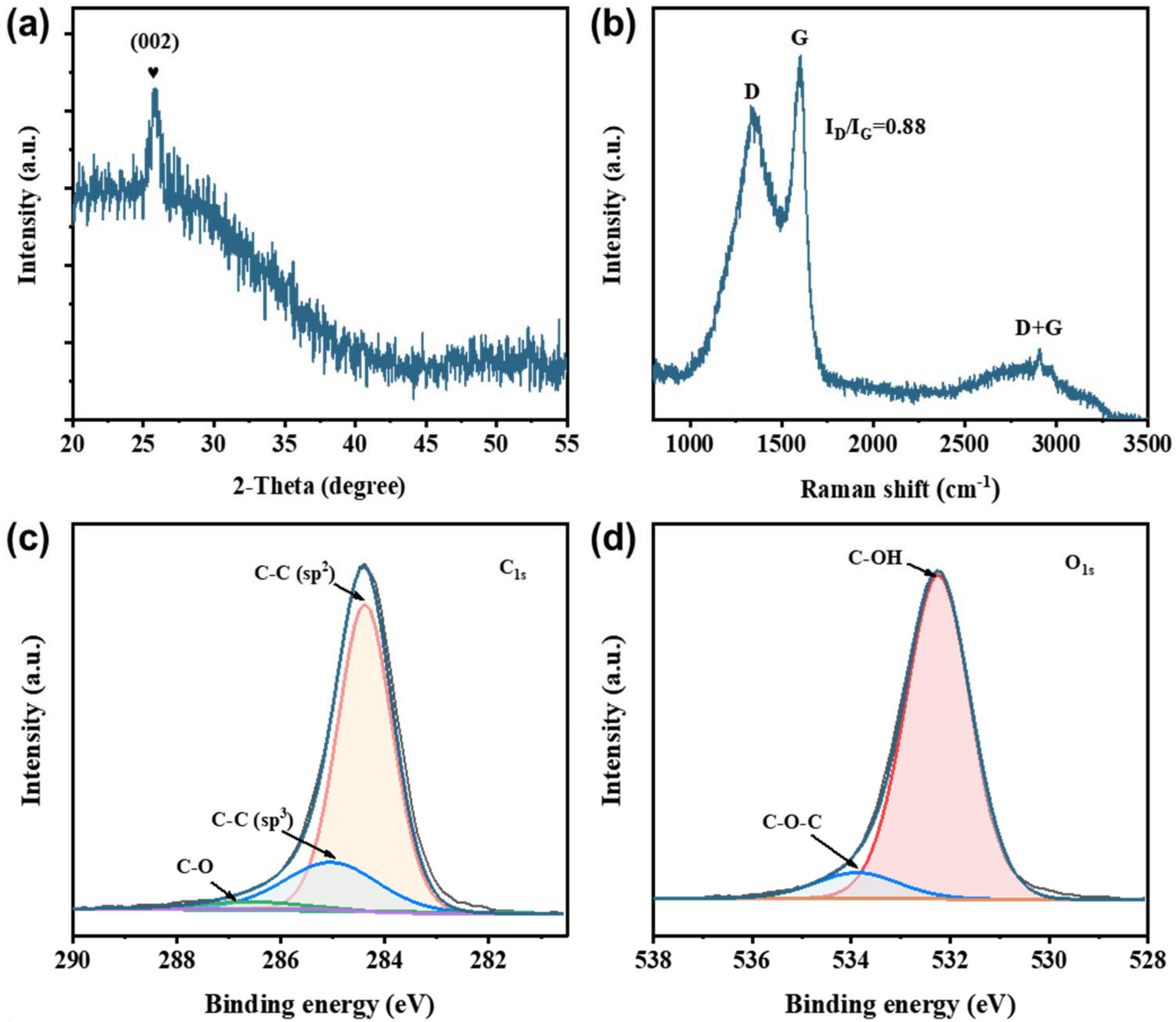

iemn
Institut d'Electronique, de Microélectronique et de Nanotechnologie
UMR CNRS 8520

Li et al. *Microsystems & Nanoengineering (2024) 10:107*

Flexible Symmetric Micro-Supercapacitors with Wide Working Voltage Window Assisted by Laser Fabrication and Liquid Crystal Gel Electrolyte

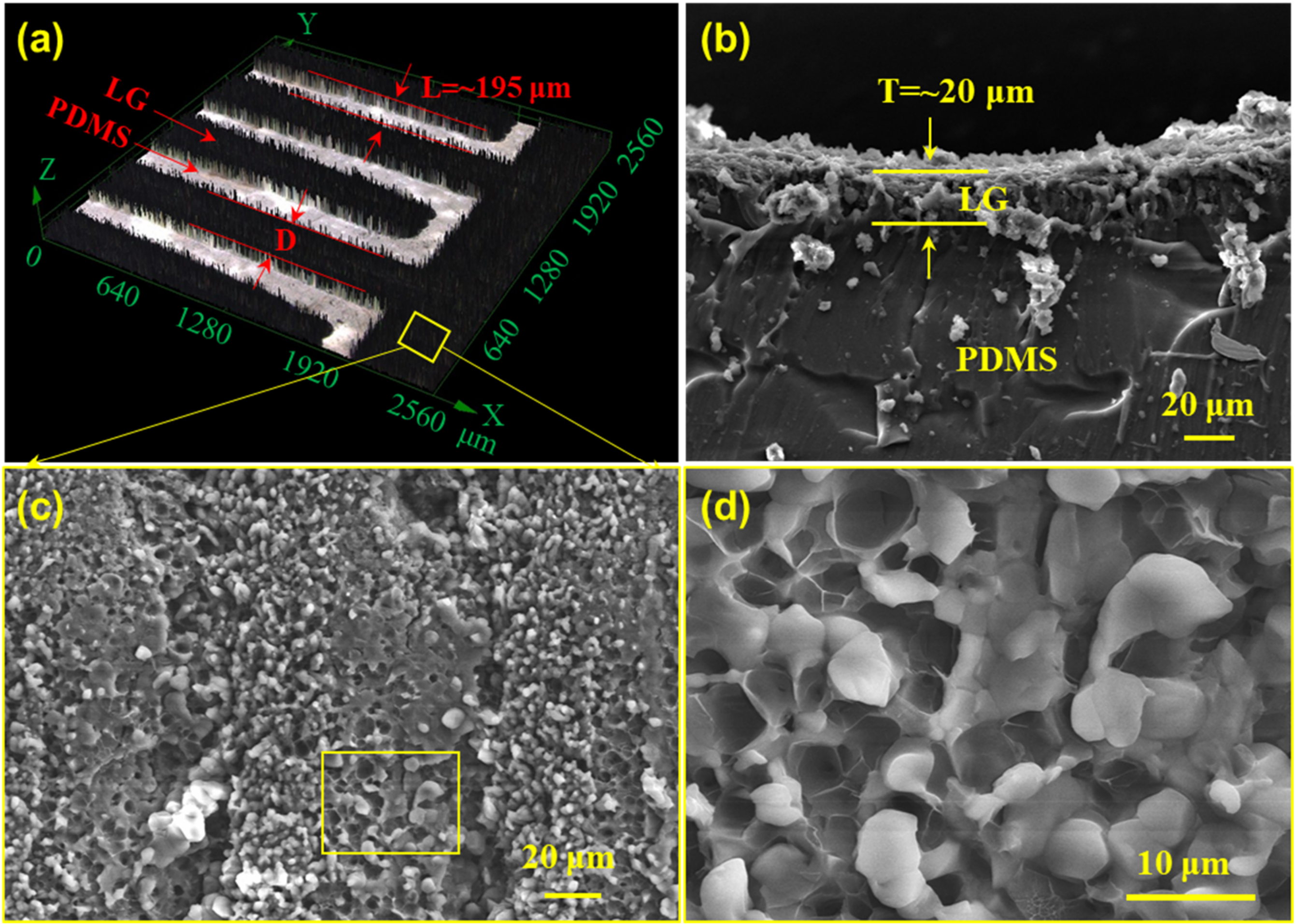

(**a**) Laser confocal scanning microscope (LCSM) image of LG-based symmetric MSC electrode . (**b**) SEM image of the cross-section morphology and (**c**, **d**) surface morphologies of the LG electrode .

iemn
Institut d'Electronique, de Microélectronique et de Nanotechnologie
UMR CNRS 8520

Li et al. ***Microsystems & Nanoengineering (2024) 10:107***

Flexible Symmetric Micro-Supercapacitors with Wide Working Voltage Window Assisted by Laser Fabrication and Liquid Crystal Gel Electrolyte

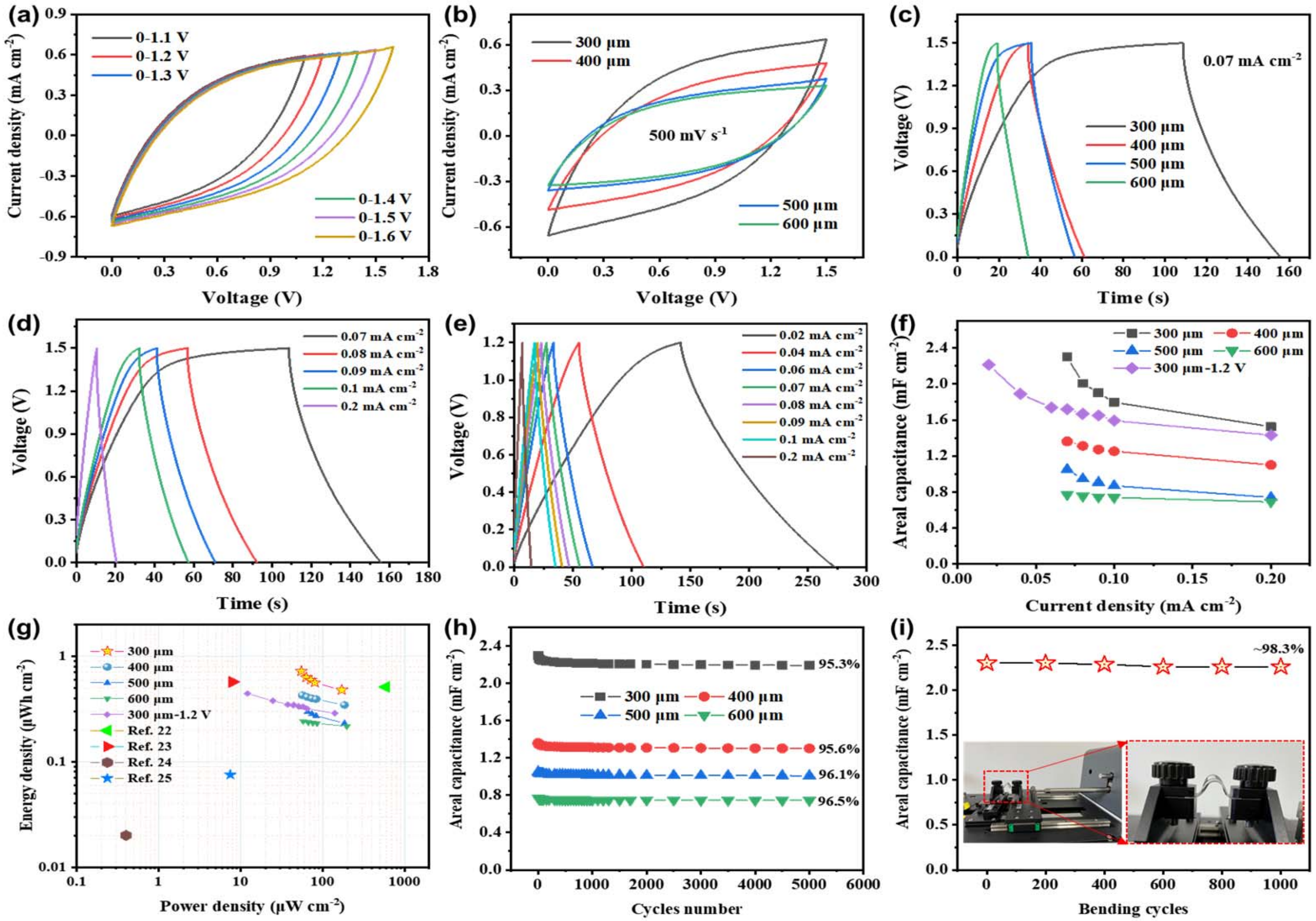

Electrochemical performance of the symmetric LG-based MSCs with PA-NI LC gel electrolyte. (**a**) CV curves of the MSC-300 device recorded at various voltage windows, (**b**) CV profiles at 100 mV·s^{-1} and (**c**) GCD plots at 0.07 mA cm^{-2} of different MSC devices, GCD curves of the MSC-300 device in the voltage window of (**d**) 0-1.5 V and (**e**) 0-1.2 V, (**f**) Areal capacitance, (**g**) Ragone Plots, (**h**) Cycling stability, (**i**) Areal capacitance measured at 0.07 mA cm^{-2} after repeat bending at 90° of the flexible MSC device

Institut d'Electronique, de Microélectronique et de Nanotechnologie
UMR CNRS 8520

Li et al. *Microsystems & Nanoengineering (2024) 10:107*

Flexible Symmetric Micro-Supercapacitors with Wide Working Voltage Window Assisted by Laser Fabrication and Liquid Crystal Gel Electrolyte

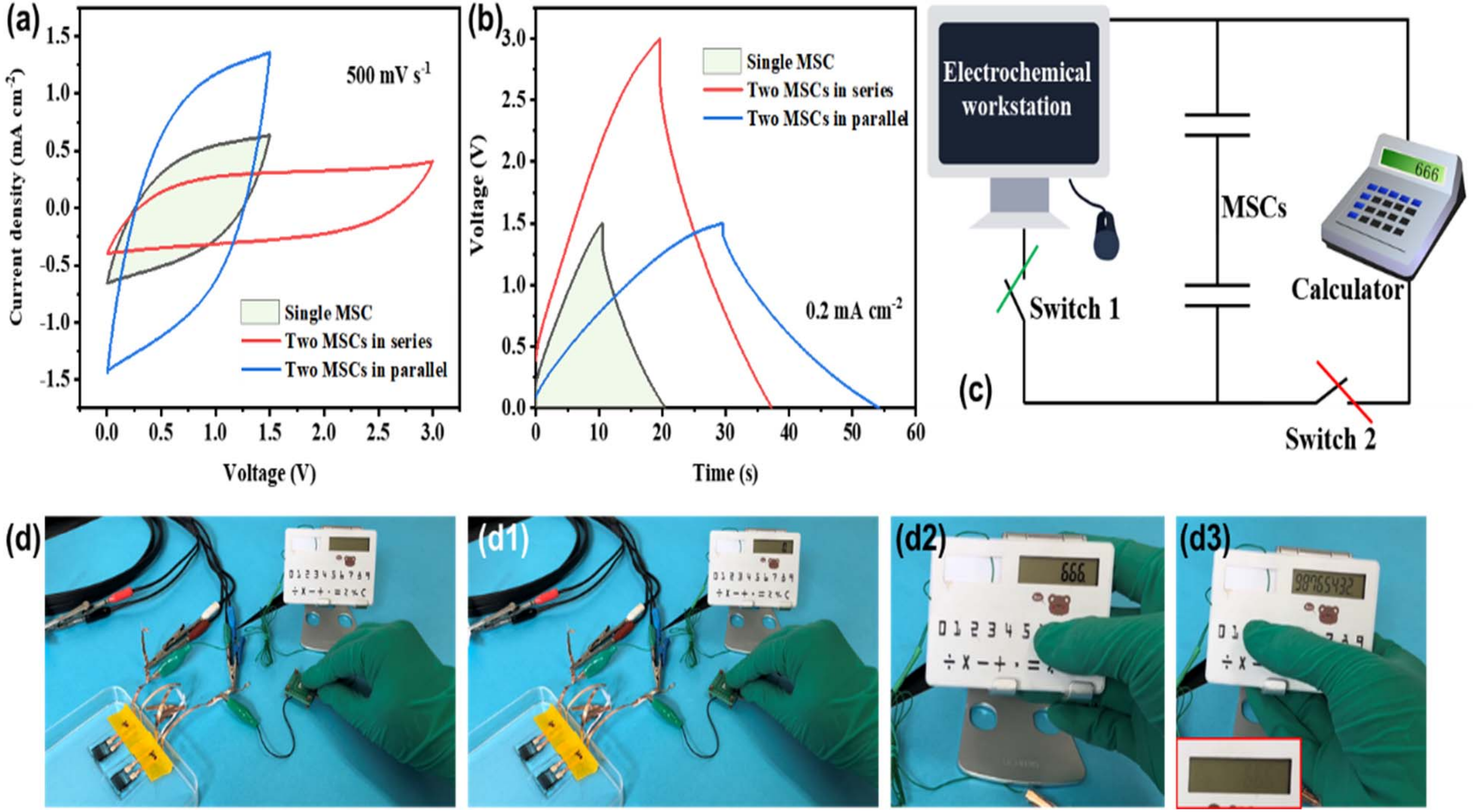

(**a**) CV curves at 500 mV s^{-1} of a single MSC-300, and two MSC-300 connected in series and parallel. (**b**) GCD plots at 0.2 mA cm^{-2} measured with PA-NI LC gel electrolyte. (**c**) Schematic equivalent circuit diagram and (**d**) photographs of the application test system

iemn
Institut d'Electronique, de Microélectronique et de Nanotechnologie
UMR CNRS 8520

Waste PET upcycling to conductive carbon-based composite through laser-assisted carbonization of UiO-66

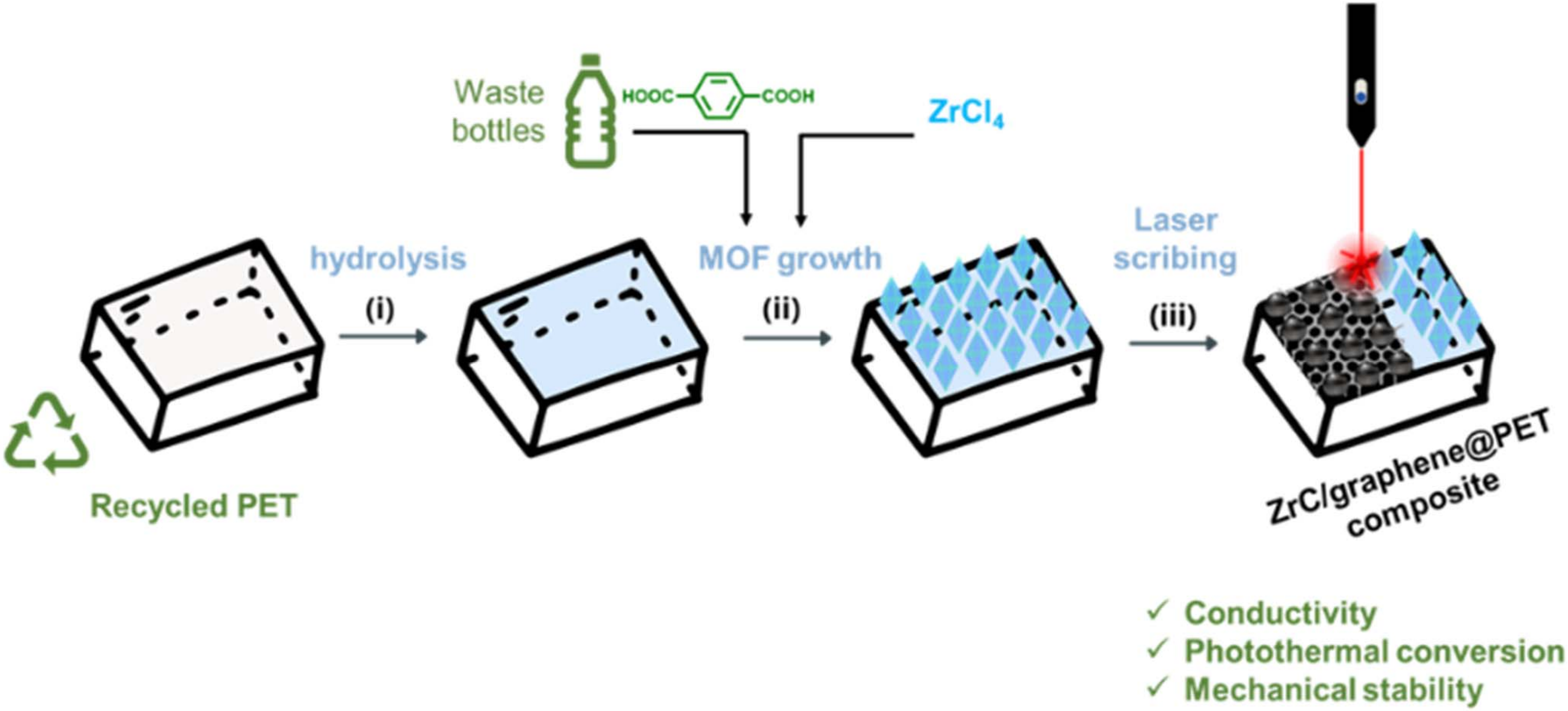

Strategy for PET@LB-UiO-66 preparation from recycled PET: (i) PET hydrolysis,
(ii) UiO-66 PET surface growth from waste PET bottle, and
(iii) laser scribing process by 405 nm irradiation.

iemn
Institut d'Electronique, de Microélectronique et de Nanotechnologie
UMR CNRS 8520

Kogolev et *al.*, J. Mater. Chem. A, 2023, 11, 1108–1115

UiO-66 (Universitetet i Oslo) MOF structure

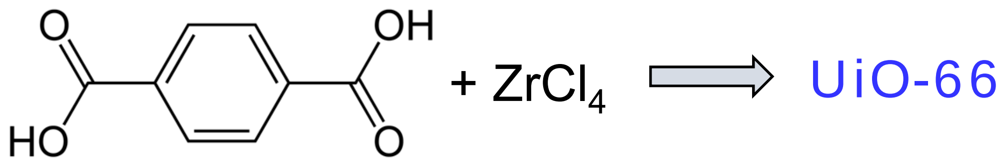

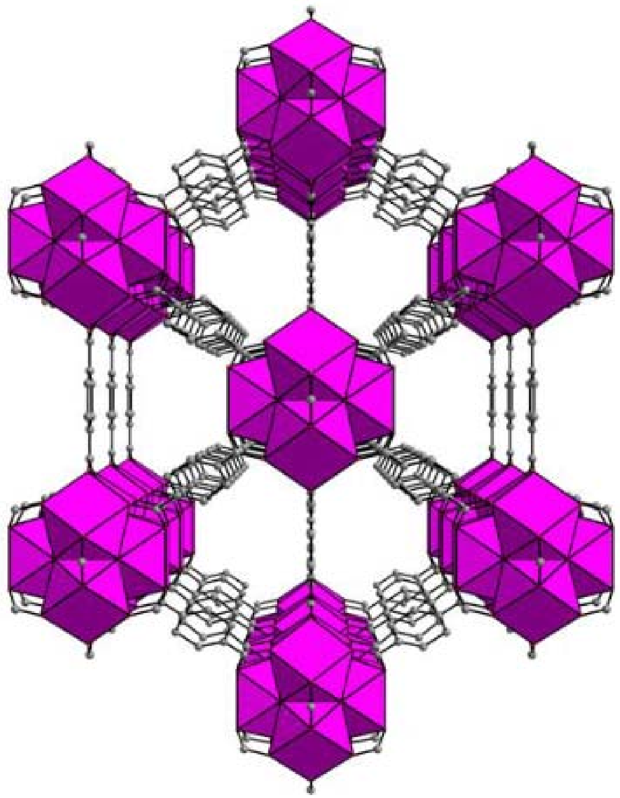

- Cheap (based on Zr^{4+} and terephthalic acid)
- High porosity
- High thermal stability
- High stability to hydrolysis
- Easy to synthesize
- Extremely versatile

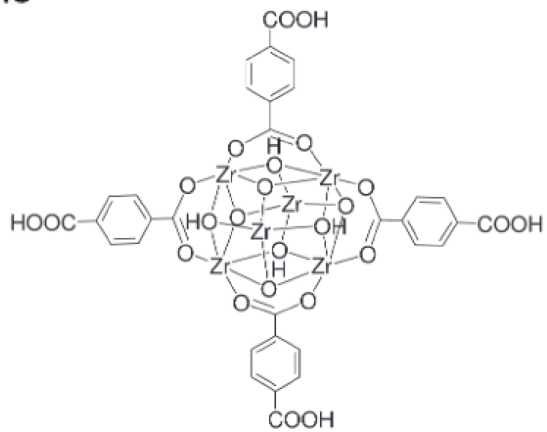

iemn
Institut d'Electronique, de Microélectronique et de Nanotechnologie
UMR CNRS 8520

The Royal Swedish Academy of Sciences has decided to award the Nobel Prize in Chemistry 2025 to

Susumu Kitagawa
Kyoto University, Japan

Richard Robson
University of Melbourne, Australia

Omar M. Yaghi
University of California, Berkeley, USA

"for the development of metal–organic frameworks"

Waste PET upcycling to conductive carbon-based composite through laser-assisted carbonization of UiO-66

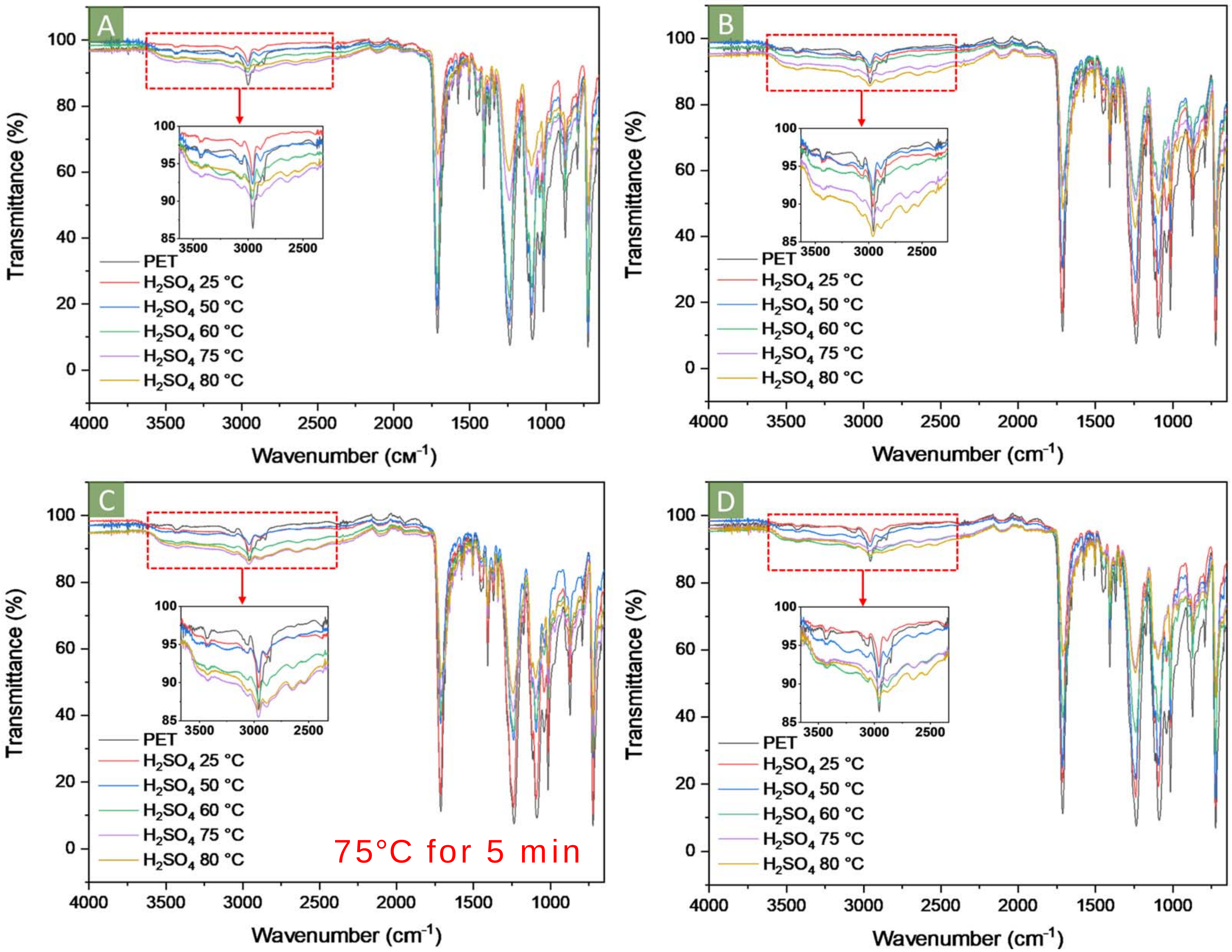

FTIR spectra of pristine and hydrolyzed PET (PET-H) plates using concentrated H_2SO_4 for (A) 1 min, (B) 2.5 min, (C) 5 min, (D) 10 min.

iemn
Institut d'Electronique, de Microélectronique et de Nanotechnologie
UMR CNRS 8520

Kogolev *et al.*, J. Mater. Chem. A, 2023, 11, 1108–1115

Waste PET upcycling to conductive carbon-based composite through laser-assisted carbonization of UiO-66

UiO-66 at 1584 and 1397 cm^{-1} due to asymmetric and symmetric stretches of COO-Zr bonds

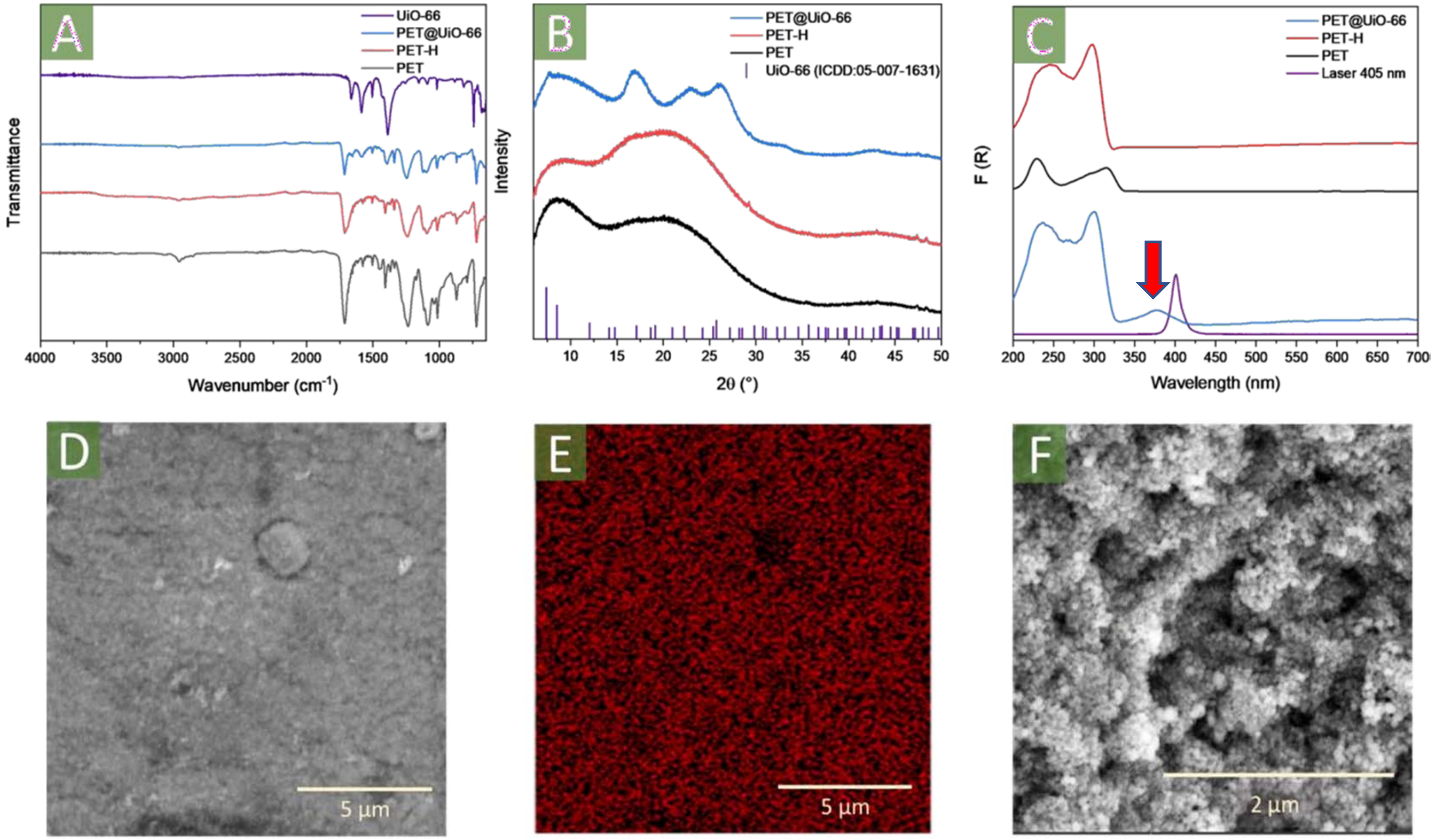

Characterization of PET@UiO-66: (A) FTIR spectra, (B) XRD patterns, (C) UV-vis spectra, (D-E) SEM-EDX map of Zr, and (F) SEM image at higher magnification

iemn
Institut d'Electronique, de Microélectronique et de Nanotechnologie
UMR CNRS 8520

Kogolev et *al.*, J. Mater. Chem. A, 2023, 11, 1108–1115

Waste PET upcycling to conducting carbon-based composite through laser-assisted carbonization of UiO-66

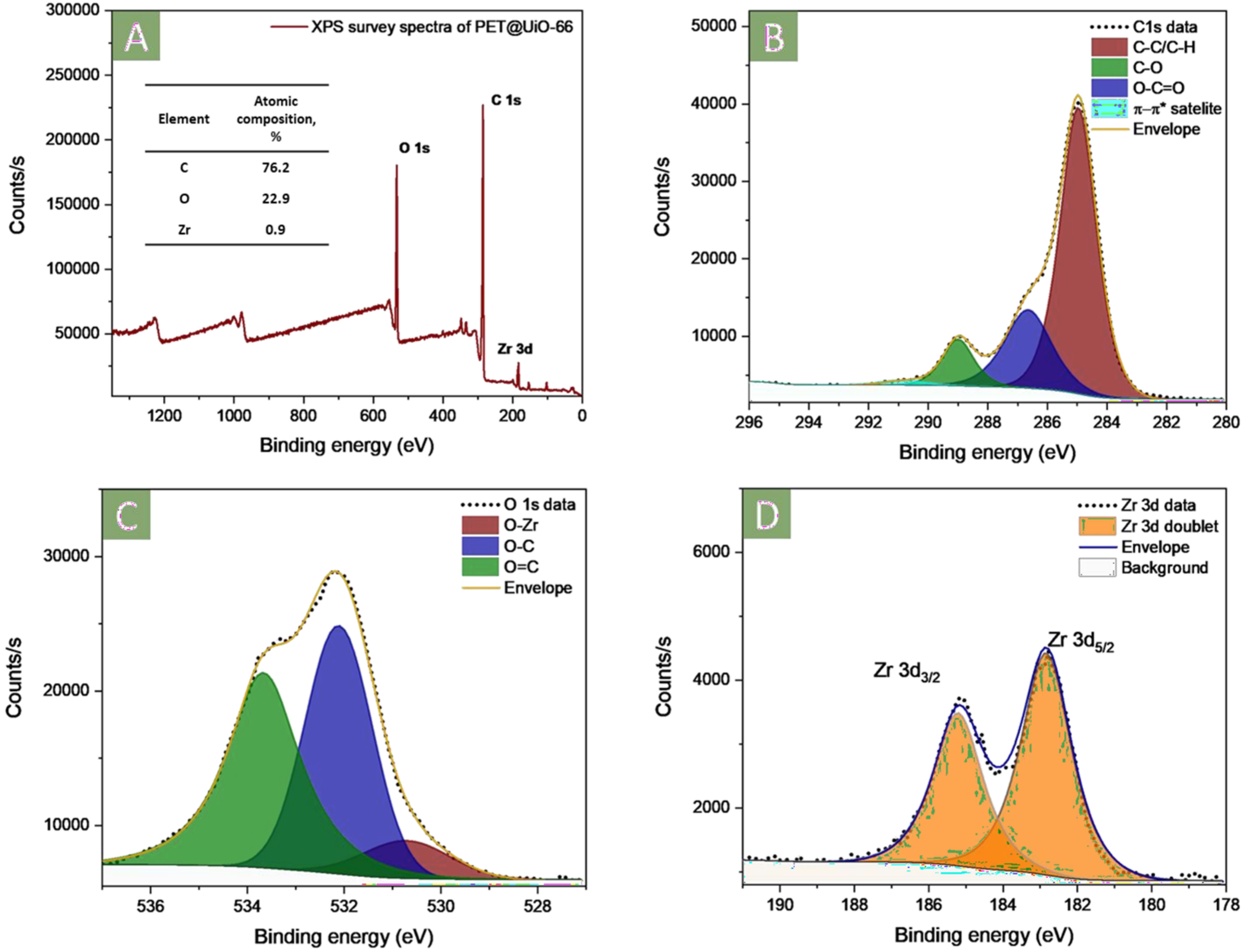

Characterization of PET@UiO-66 by XPS: (A) Survey spectrum, (B) C 1s, (C) O 1s, and (D) Zr 3d regions

iemn
Institut d'Electronique, de Microélectronique et de Nanotechnologie
UMR CNRS 8520

Kogolev *et al.*, J. Mater. Chem. A, 2023, 11, 1108–1115

Preparation of PET@LB-UiO-66

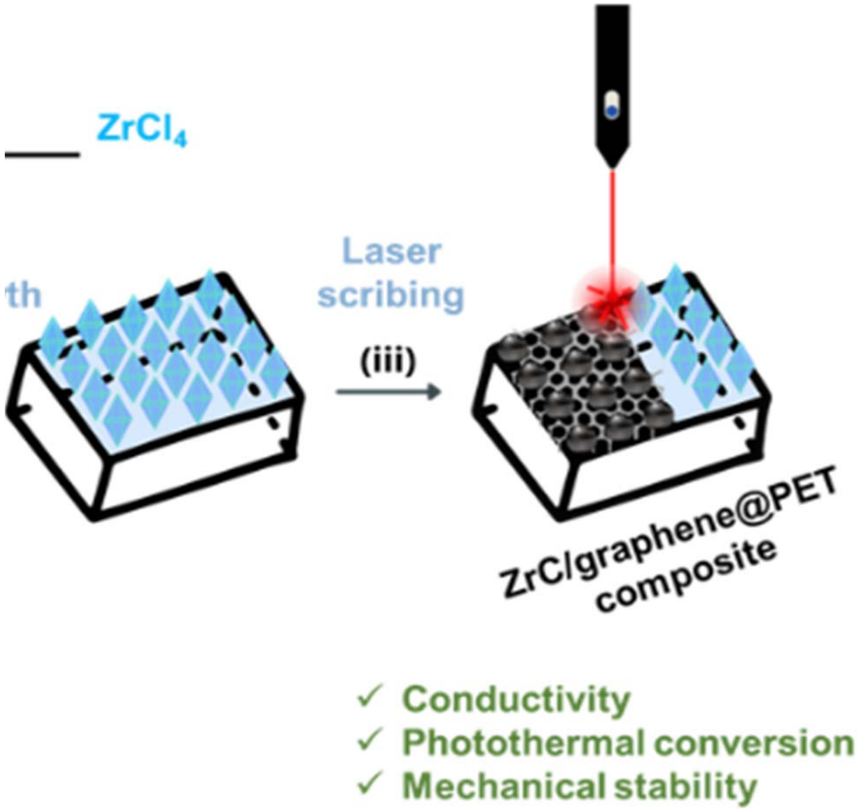

iemn Institut d'Electronique, de Microélectronique et de Nanotechnologie UMR CNRS 8520

Laser processing was carried out using a pulsed diode laser NEJE DK-8-KZ at a wavelength of 405 nm on the 1 cm^2 PET@UiO-66 area. The laser was operated at a pulse frequency of 1.6 kHz and rated power of ~1.6 W. To carry out the process, the laser beam was focused on the material, and irradiation was carried out when the laser moved along the plate. In our laser control system, the average power was varied by controlling the laser pulse time and frequency. The software allowed us to control two parameters – "P" (power) and "D" (depth). The "P" parameter controlled the pulse duration, while "D" set the pulse frequency (laser beam velocity). **Optimization of the carbonization process** was carried out using the **Nelder-Mead** method by varying parameters "P" and "D" in the software of the laser system. For carbonization of UiO-66 on the surface, the following optimized parameters were subsequently used: 49 % power from nominal (735 mW), 26 % depth (9.0 mm/s).

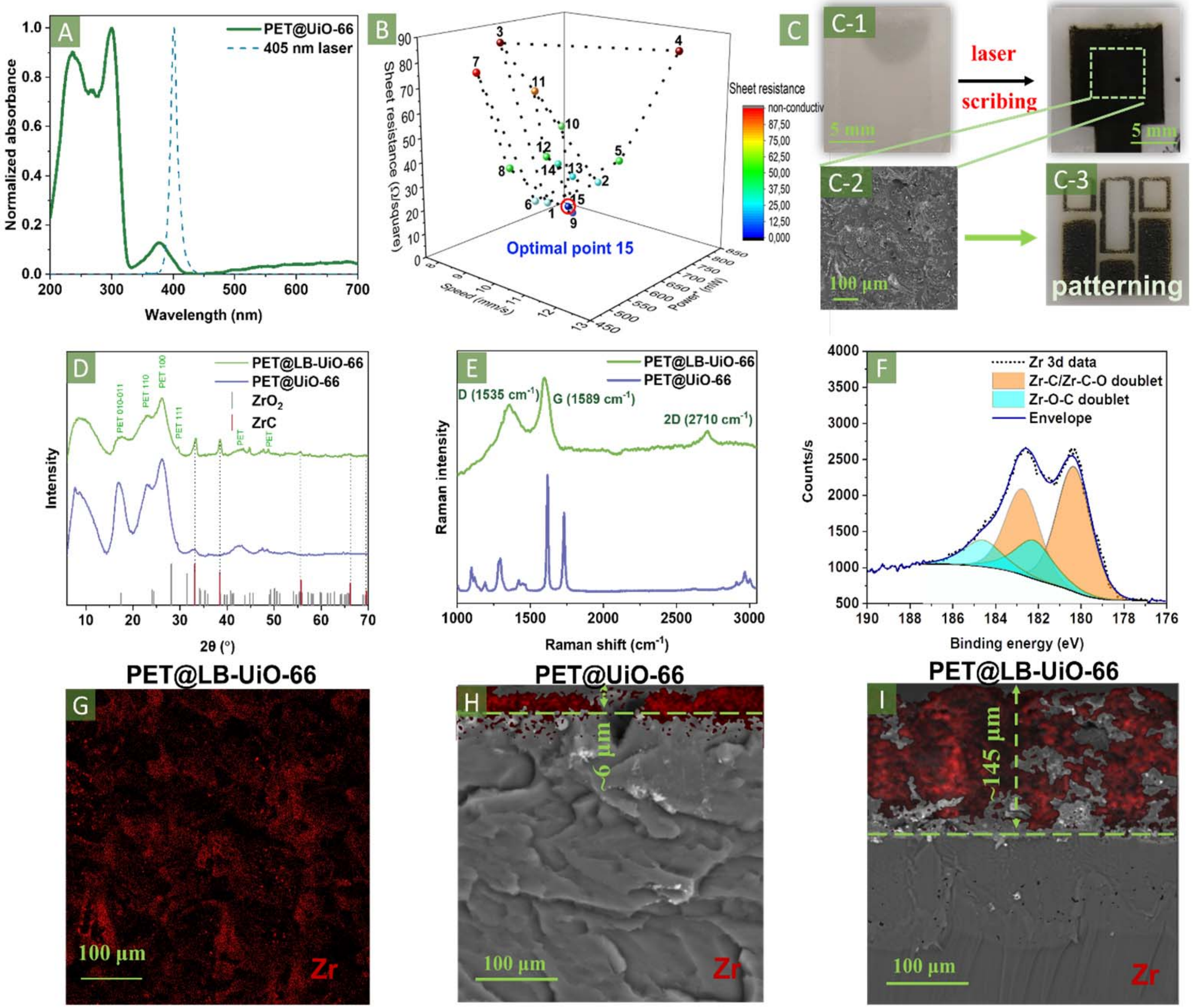

(A) UV-vis spectrum of PET@UiO-66. (B) Optimization of PET@UiO-66 carbonization by the Nelder-Mead Method; *Nominal laser power. (C) Material images before and after laser treatment, where C-1 is a general view, C-2 – SEM of PET@LB-UiO-66 after treatment under optimal conditions, C-3 – Optical image of the pattern (Logo Tomsk Polytechnic University) prepared by PET@UiO-66 laser scribing. Characterization of PET@LB-UiO-66: (D) XRD patterns, (E) Raman spectra, (F) Zr 3d XPS spectrum, (G) EDX mapping of Zr from image on C-2, cross-sectional SEM-EDX images of (H) PET@UiO-66 and (I) PET@LB-UiO-66.

Waste PET upcycling to conducting carbon-based composite through laser-assisted carbonization of UiO-66

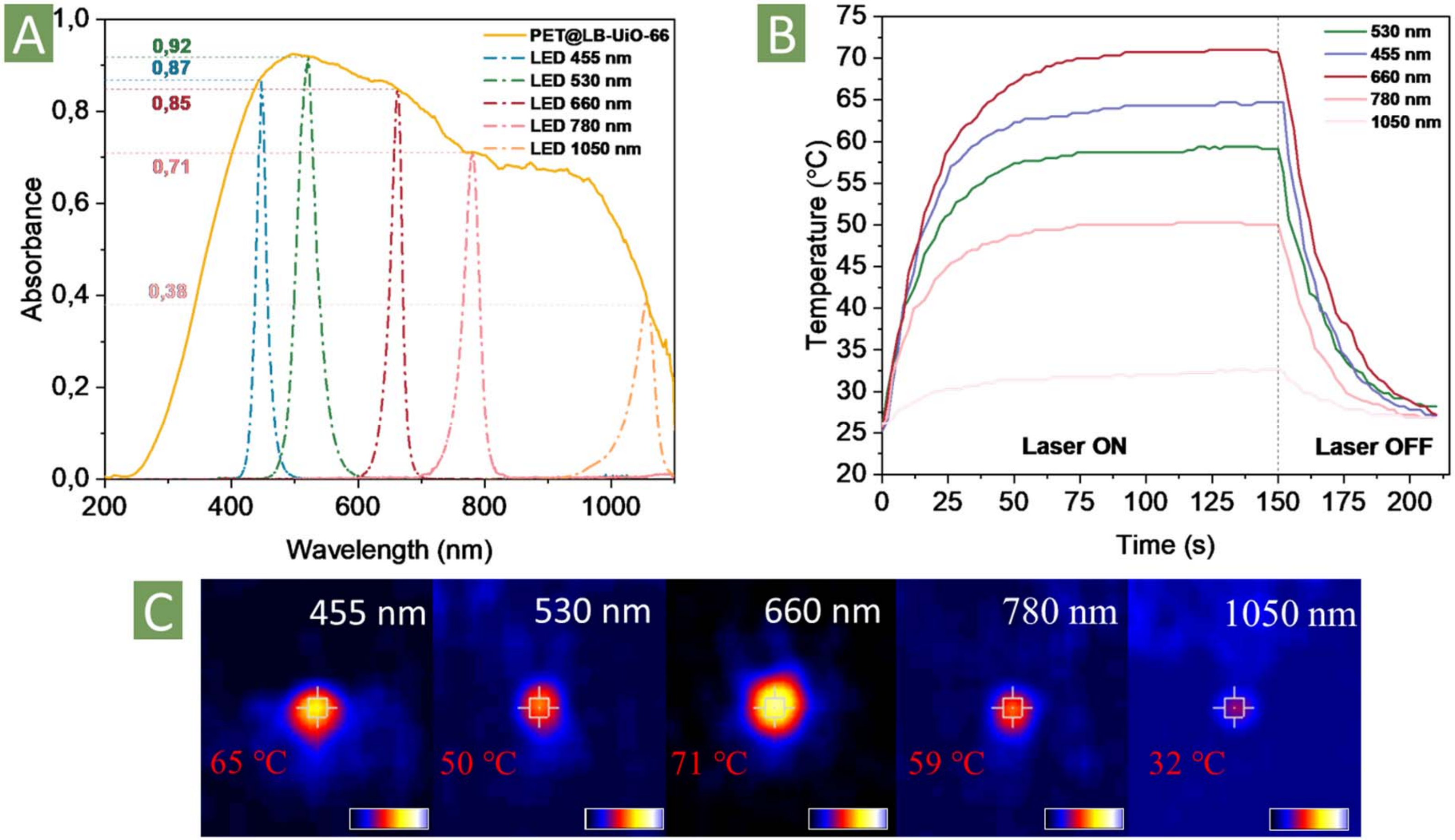

(A) UV-vis spectrum of PET@LB-UiO-66 with spectra of LED sources. (B) Photothermal curves of PET@LB-UiO-66 acquired at 5 different wavelengths. (C) Images taken using a thermal camera during LED irradiation of PET@LB-UiO-66 at 5 different wavelengths.

iemn
Institut d'Electronique, de Microélectronique et de Nanotechnologie
UMR CNRS 8520

Kogolev et *al.*, J. Mater. Chem. A, 2023, 11, 1108–1115

Waste PET upcycling to conducting carbon-based composite through laser-assisted carbonization of UiO-66

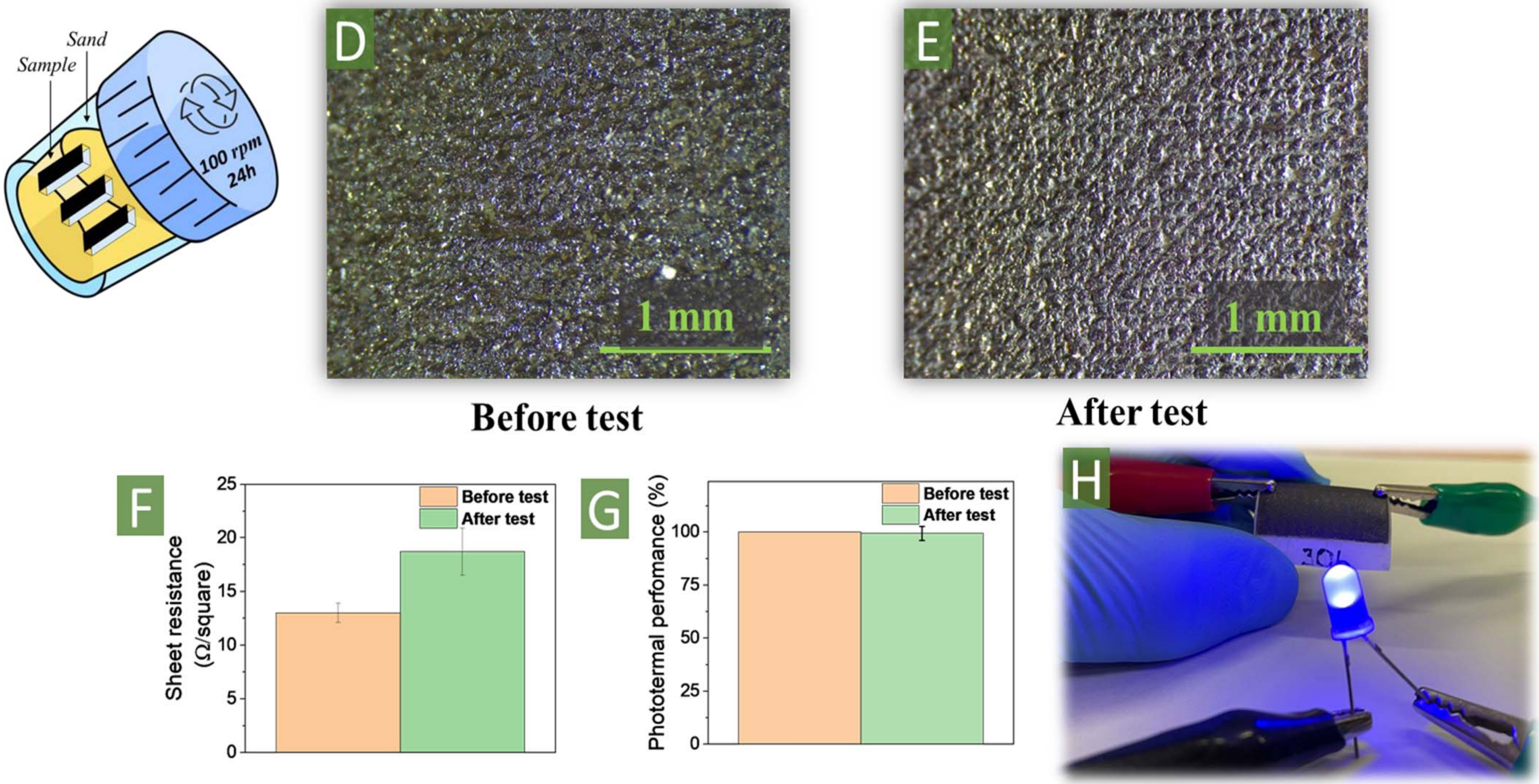

Optical microscopic photos: (D) Before mechanical test, (E) after mechanical test. Comparison diagram of (F) sheet resistance and (G) photothermal performance before and after mechanical test. (H) Photo of bent PET@LB-UiO-66 used as conductor to power LED.

iemn
Institut d'Electronique, de Microélectronique et de Nanotechnologie
UMR CNRS 8520

Kogolev et *al.*, J. Mater. Chem. A, 2023, 11, 1108–1115

iemn Institut d'Electronique, de Microélectronique et de Nanotechnologie UMR CNRS 8520

https://www.longsingtechnology.com/hybrid-supercapacitors/

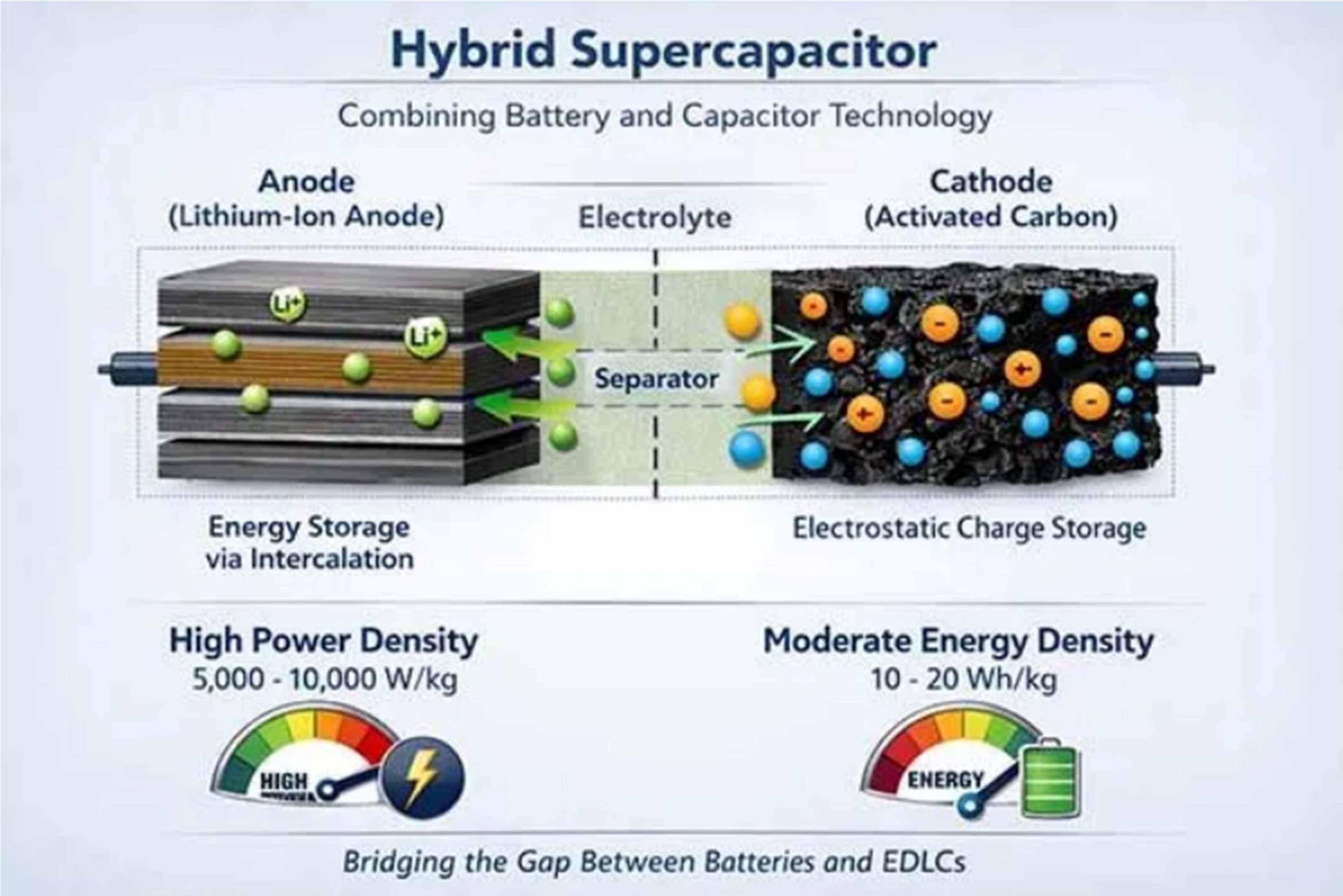

https://www.longsingtechnology.com/hybrid-supercapacitors/

Parameter	Lithium-Ion Battery	Hybrid Supercapacitor	Standard EDLC
Power Density	100-300 W/kg	5,000-10,000 W/kg	10,000-15,000 W/kg
Energy Density	150-250 Wh/kg	10-20 Wh/kg	5-8 Wh/kg
Cycle Life	500-2,000 cycles	1,000,000+ cycles	1,000,000+ cycles
Charge Time	1-4 hours	10-60 seconds	1-10 seconds
Operating Temperature	-20°C to +60°C	-40°C to +85°C	-40°C to +65°C

Cost considerations extend beyond purchase price. The initial cost per watt-hour for a hybrid supercapacitor battery exceeds that of batteries.

However, lifetime cost calculations change the picture. Divide total cost by cycle life and the hybrid solution often wins. A $50 hybrid device lasting 1 million cycles costs $0.00005 per cycle. A $20 battery lasting 1,000 cycles costs $0.02 per cycle. For high-cycle applications, the economics clearly favor hybrid technology.

Real-world validation matters more than datasheets. We recently worked with a Japanese customer installing sensors for remote mountain monitoring. The application demanded 15-year maintenance-free operation in temperature extremes from -40°C to +70°C.

Bio-based electrolytes for supercapacitors: A sustainable path toward green energy storage

A summary of the most suitable electrolyte for a specific supercapacitor device need

Primary device need	Most suitable bio-electrolyte class	Reason	Typical device targets
Low cost, safety, high power, flexible, and wearable devices	Biopolymer hydrogels/GPEs	High ionic conductivity, aqueous safety, and simple processing	Wearable electronics, flexible and printable supercapacitors, disposable or short-lifetime energy storage
Flexibility, wide temperature range, and solid-state operation	Bio-derived Eutectogels (DES-based)	Non-volatile, anti-freezing, mechanically robust	outdoor electronics, automotive and industrial sensors, flexible solid-state supercapacitors
High voltage, high energy density	Bio-ionic liquids / ILCs	Wide electrochemical stability window	high-energy supercapacitors, hybrid battery–capacitor systems, and stationary or high-end devices
Balanced performance, multifunctionality, and tunability	Hybrid bio-electrolytes	Combine conductivity, voltage, and mechanics	next-generation flexible electronics, high-performance solid-state supercapacitors, multifunctional devices (self-healing, antifreeze, recyclable)

DES = deep eutectic solvent; GPEs = gel polymer electrolytes; ILCs = ionic liquid crystals.

iemn
Institut d'Electronique, de Microélectronique et de Nanotechnologie
UMR CNRS 8520

Next Energy 12 (2026) 100627

Acknowledgment

Dr. Zhihao Wu

Univ. Lille, CNRS, Univ. Polytechnique Hauts-de-France, UMR 8520 - IEMN, F-59000 Lille, France

Dr. Min Li

[1] State Key Laboratory for Manufacturing Systems Engineering, International Joint Laboratory for Micro/Nano Manufacturing and Measurement Technologies, Xi'an Jiaotong University, Xi'an 710049, China.

D. Yurdanur Türker, Mert Umut Özkaynak and D. Koray Bahadır Dönmez

Sabanci University, Nanotechnology Research and Application Center (SUNUM), Istanbul, Turkey.

Chinese Scholarship Council (CSC)

LEAP-RE **2022 - 2025**
Long-Term Joint EU-AU Research and Innovation Partnership on Renewable Energy

LEAP-SE **2026 - 2029**

iemn Institut d'Electronique, de Microélectronique et de Nanotechnologie UMR CNRS 8520

AU - EU Collaborative Research and Innovation Projects on Sustainable Energy